

Lars-Adrian Amundsen

Evaluation of a reversible NH₃ heat pump unit

Masteroppgave i Energi og Miljø

Veileder: Armin Hafner

Juni 2019

Lars-Adrian Amundsen

Evaluation of a reversible NH₃ heat pump unit

Masteroppgave i Energi og Miljø
Veileder: Armin Hafner
Juni 2019

Norges teknisk-naturvitenskapelige universitet
Fakultet for ingeniørvitenskap
Institutt for energi- og prosesssteknikk



Preface

This master thesis is the conclusion of my Master of Science degree in Energy and Environmental Engineering with the Department of Energy and Process Engineering at the Norwegian University of Science and Technology (NTNU). This report is a continuation of the project work done during the fall of 2018. The thesis is an evaluation of a reversible NH₃ heat pump installed at the offices of GK in Bergen. The aim is to investigate potential changes which could improve the efficiency of the system. The work was supervised by professor Armin Hafner from the Department of Energy and Process Engineering NTNU.

I would like to express my sincerest gratitude to Armin Hafner for his guidance through the process of creating this report. I would also like to thank Gert Nielsen for sharing his expertise on the subject of this heat pump and Tom Svendsen for giving me access to all the data necessary to evaluate the system. Lastly, I would like to thank my sister Rannveig Amundsen and my father Magne Amundsen for helping me proofread the report.

Trondheim, 10.06.2019

Lars-Adrian Amundsen

Abstract

This report examines a NH_3 heat pump unit that is installed at GK's offices at Folke Bernadottes Vei 40 in Bergen, Norway. The report seeks to present relevant information about the heat pump to better understand the system, and subsequently make models to simulate the system to evaluate its performance.

The models that have been employed as the basis for the simulations have been designed in Modelica, a simulation program with specialized heat pump applications. The models of the system are simplified versions of the real heat pump, and does not take into account all of the different components of the real system. The simulations primarily seek to establish the performance of the system in single-stage compression, and to find what the performance would be if it instead was using two-stage compression with different configurations and ambient conditions.

The results found in this report indicate that the performance of the system could be improved slightly by changing the settings of when the heat pump should use two-stage rather than single-stage compression. The level of potential energy- and economical savings indicated by these findings, however, appear too slim to warrant spending resources on making the necessary changes to the system.

Sammendrag

Denne rapporten er laget for å evaluere en reversibel NH_3 varmpumpe som GK har installert i sitt kontorbygg i Folke Bernadottes Vei 40 i Bergen. Rapporten tar for seg teoretisk bakgrunnsmateriale relevant for NH_3 -systemer, beskriver varmpumpen og viser resultatene av simuleringer av varmpumpen ved ulike driftsmoduser.

Modellene er laget i simuleringsverktøyet Modelica. Hovedfokuset har vært å lage modeller som simulerer de faktiske forholdene ved anlegget for å vurdere om varmpumpen fungerer som den skal, og å simulere to-steps kompresjon for å finne potensiell energibesparelse ved å bruke to-steps kompresjon mer enn tilfellet er i dag. For å finne COP-verdien, også kalt effektfaktoren, har simuleringer blitt gjort for å finne kjøle- og varmebidraget fra varmpumpen, massestrømmen til kjølemediet gjennom systemet og entalpiverdier ved ulike stadier i syklusen.

Resultatene som er presentert i rapporten gir en klar indikasjon på at det å bruke to-steps kompresjon ved andre tilfeller enn kun når utetemperaturen er lavere enn -10°C , som er innstillingen som brukes i dag, vil spare energibruken til kompressorene. Den potensielle energibesparelsen funnet fra simuleringene er dog ikke stor nok til å rettferdiggjøre å bruke ressurser på å endre systemet.

Contents

1	Introduction	10
1.1	Background	10
1.2	Problem Formulation	10
1.3	Structure of the report	11
2	Literature Review	13
2.1	Vapour compression NH_3 heat pump for high temperature heating	13
2.2	Ground Source Heat Pumps using NH_3	15
2.3	Small ammonia heat pumps for space and hot tap water heating	17
3	Theory	18
3.1	Basic principle of the refrigeration cycle	18
3.1.1	Isentropic efficiency	20
3.1.2	Volumetric efficiency	20
3.2	Ammonia as a working fluid	21
3.2.1	GWP and ODP	22
3.2.2	Toxicity and flammability	22
3.2.3	Corrosion	22
3.3	Piston compressors	23
3.3.1	Part Load	25
3.4	Desuperheater	26
3.5	Air cooled Condensers	28
3.6	Modelica	29
4	Description of the system	30
4.1	Compressors	32
4.2	Heat exchangers	33
5	Model	34
6	Results	40
6.1	16th of May 2019	40
6.1.1	Heating	41
6.1.2	Cooling	46
6.2	28th of January 2019	50
6.2.1	Heating mode	51

6.2.2	Cooling Mode	54
7	Discussion	59
7.1	Single-stage versus two-stage compression	59
7.2	Compressor heat loss	59
7.3	Secondary fluid flow rate	60
7.4	Economic evaluation	60
8	Conclusion	63
9	Recommendations for Future Work	65
A	Components in Modelica	69
A.1	Air heat exchanger in model	69
A.2	Condenser in heating mode	70
A.3	Evaporator in cooling mode	72
A.4	Compressor	74
A.5	PI-controller	75
B	Results from ClimaCheck	77
B.1	16th of May	77
B.2	28th of January	80
C	Design values for the heat pump at Folke Bernadottes Vei 40	82
D	Heat pump function description	83
E	PI-diagram of heat pump	87
F	Heat exchanger in the heat pump	89
G	Compressor in the heat pump	92
H	Risk assessment	95

List of Figures

1	Simplified principle of the Drammen heat pump schematics . . .	14
2	Log Ph diagram of ammonia showing high compressor discharge temperature optimized for heating.	14
3	Compression-absorption	16
4	Principle sketch of a refrigeration cycle	18
5	Compressor efficiency at different compression ratios with ammonia as refrigerant with different rotational speed, n (rpm) . .	24
6	Compressor efficiency at part load	25
7	Effects on the power ratio results from different capacity control methods.	26
8	LogP-h diagram of a heat pump with two stage compression and interinjection desuperheating	27
9	T-s diagram of an ammonia heat pump with two stage compression and interinjection desuperheating	28
10	Heat pump system at Folke Bernadottes Vei 40	30
11	Heat pump in heating mode	31
12	Heat pump in cooling mode	32
13	Model of the heat pump in single-stage heating mode	35
14	Model of the heat pump in single-stage cooling mode	36
15	Model of the heat pump in two-stage heating mode	38
16	Model of the heat pump in two-stage cooling mode	39
17	Some values from ClimaCheck for the 16th of May	41
18	Mass flow of refrigerant through the condenser with single-stage and two-stage compression	42
19	Heating capacity of the heat pump with single-stage and two-stage compression	43
20	Compressor work in single-stage and two-stage mode	44
21	Log Ph diagram of the single-stage cycle	45
22	Log Ph diagram of the two-stage cycle	45
23	Mass flow of refrigerant through the evaporator with single-stage and two-stage compression	47
24	Cooling capacity of the heat pump with single-stage and two-stage compression	48
25	Compressor work in single-stage and two-stage mode	48

26	Log Ph diagram of the single-stage cycle	49
27	Log Ph diagram of the two-stage cycle	49
28	Average delivered heating and cooling compared to the compressor work	50
29	Heating capacity of the heat pump with single-stage and two-stage compression	52
30	Compressor work in single-stage and two-stage mode	52
31	Log Ph diagram of the single-stage cycle	53
32	Log Ph diagram of the two-stage cycle	54
33	Cooling capacity of the heat pump with single-stage and two-stage compression	55
34	Compressor work in single-stage and two-stage mode	56
35	Log Ph diagram of the single-stage cycle	57
36	Log Ph diagram of the two-stage cycle	57
37	Average delivered heating and cooling compared to the compressor work	58
38	Compressor work for a month from ClimaCheck	61

List of Tables

1	Comparison on different refrigerants physical properties.	21
---	---	----

Nomenclature

GWP – Global Warming Potential

ODP – Ozone Depletion Potential

IDLH – Immediately Dangerous to Life or Health

NBP – Normal Boiling Point

NWF – Natural Working Fluid

HTHP – High Temperature Heat Pump

GSHP - Ground-Source Heat Pump

COP - Coefficient of Performance

CFC - Chlorofluorcarbon

HCFC - Hydro-chlorofluorcarbon

HFC - Hydrofluorcarbon

DHW - Domestic Hot Water

RPM - Revolutions Per Minute

\dot{m} - Mass Flow

\dot{V} - Volume Flow

\dot{Q} - Heat Flow

\dot{W} - Work

π - Pressure Ratio

η - Efficiency

η_{is} - Isentropic Efficiency

λ - Volumetric Efficiency

ν - Specific Volume

h_i - Enthalpy at state i

NH₃ - Ammonia

R717 - Ammonia

SPF - Seasonal Performance Factor

n - Rotational Speed of Compressor

P - Pressure

T - Temperature

T_{cond} - Condensation Temperature

T_{evap} - Evaporation Temperature

T_{crit} - Critical Temperature

$T_{\text{comp.out}}$ - Compressor Outlet Temperature/Discharge Gas Temperature

1 Introduction

1.1 Background

The global climate is changing at a rapid pace (United Nations, 2019). This brings a variety of challenges, one being the increasing need for efficient systems for heating and cooling of buildings. The energy spent for heating of buildings in Norway yearly is 80 TWh (NOVAP). Heat pumps are an integral part of lowering the energy usage for heating purposes. Historically, there have been a number of different refrigerants used in heat pumps. Chlorofluorocarbons (CFC) and Hydro-chlorofluorocarbons (HCFC) used to be popular as refrigerants, but they have a devastating effect on the ozone layer. Therefore, in 1987, the Montreal Protocol was signed, with the intention of phasing out these refrigerants. Hydrofluorocarbons (HFC) have been very popular since then, but these refrigerants have very high GWP-values. The Montreal Protocol was upgraded in 2016 to make sure these refrigerants are phased out to about 15% of the current amount before 2040 (United Nations, 2016).

Natural working fluids have gained popularity in recent years because of their low global warming potential (GWP) and ozone depletion potential (ODP) values. Optimization of these heat pumps can contribute to even larger energy savings, which will have an impact on the carbon footprint of the given building, and will also benefit the tenants economically.

1.2 Problem Formulation

GK Norge has a reversible ammonia (NH_3) heat pump in their head office in Folke Bernadottesvei 40, Bergen. The heat pump system is designed as a two-stage unit which supports the entire building (heating and cooling).

The system has to operate at various operating conditions, however, part load has the dominant share. The ammonia heat pump unit can be operated either in a single-stage mode or two-stage mode. An evaluation of today's control deciding which mode is applied should be part of the project work. This will enable the candidate to propose potential optimisations of the control, based on predicting the economic benefits of an upgrade. Another topic could be

a potential integration of a desuperheater downstream of the first compressor stage, this will reduce the condensing pressure when heating and cooling is provided simultaneously.

The unit is equipped with a performance analysis and logging system from ClimaCheck. Data gathered from this system should be examined by the candidate. A theoretical / economical comparison of air cooled condensers (with liquid drain by gravity) in comparison to standard condensers should be performed to understand consequences of this design decision.

The following tasks are to be considered:

1. Literature review on NH₃ heat pump systems.
2. Prepare HSE for the field tests.
3. Describe the energy systems of the building with focus on the heat pump unit.
4. Develop simplified model of the plant (Modelica) to enable a performance analysis.
5. Propose potential system updates to reduce the primary energy use and the economic benefits.
6. Project report including results, summary, discussion and conclusions.
7. Draft version of a scientific paper.
8. Make proposal for further work.

1.3 Structure of the report

Chapter 1: Introduction. Will give a basic overview of the topic discussed in the report, as well as the scope of the work.

Chapter 2: Literature Review. Will look at the state of NH₃ heat pumps at the present time.

Chapter 3: Theory. Presents theory relevant for ammonia and heat pumps in general.

Chapter 4: Description of the system. Will provide a description of the ammonia heat pump installed at GKs offices in Folke Bernadottes Vei 40 in Bergen, Norway.

Chapter 5: Model. Presents the simplified models of the system.

Chapter 6: Results. Will present results from simulations of the model.

Chapter 7: Discussion. In this section, the results from the simulations will be analysed.

Chapter 8: Conclusion. In this section, conclusions that can be derived from the results will be presented.

Chapter 9: Recommendations for Future Work. This section will give recommendations for further work within this topic that could provide more in depth results and potential recommendations for system improvements.

2 Literature Review

2.1 Vapour compression NH₃ heat pump for high temperature heating

Ammonia has been widely used as a refrigerant for heating and cooling applications. It has especially been useful in processes with large energy requirements. Because of the high compressor discharge temperature of ammonia at high pressures, combined with a high pressure of 60 bar for a condensation temperature of 97.5° C, the potential for usage in HTHPs has been limited. (Stene, 2008) and (Palm, 2008) investigated the possibility of using ammonia as the refrigerant for low capacity domestic hot water heat pumps, but the discharge temperature of the heat sink was below 80 degrees.

In 2018, (Bamigbetan et al., 2017) investigated the possibility of utilizing the de-superheating region more efficiently to get a higher heat sink outlet temperature without having to increase the condensation temperature. The high compressor discharge temperature can be utilized to achieve a 90° C or higher hot water temperature. This has been shown by (Hoffmann and Pearson, 2011) with a NH₃ heat pump installed in Drammen, Norway.

A sketch showing the basic principle of the heat pump is showed in figure 1. The condensation temperature is just below 90° C, but by utilizing de-superheating and intercooler heat combined with the heat of condensation, a hot water temperature of 90° C is achieved (Bamigbetan et al., 2017). Figure 2 shows this process in a Log Ph diagram.

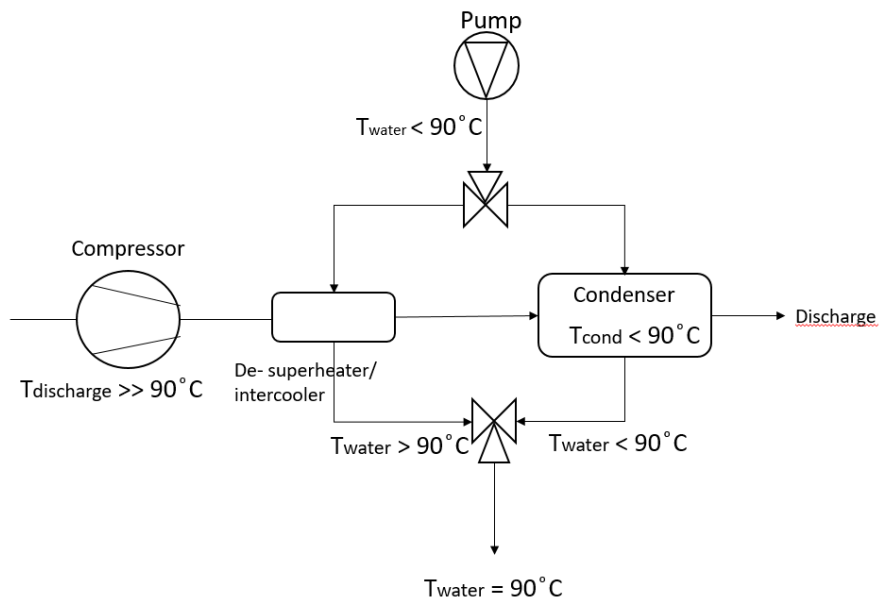


Figure 1: Simplified principle of the Drammen heat pump schematics

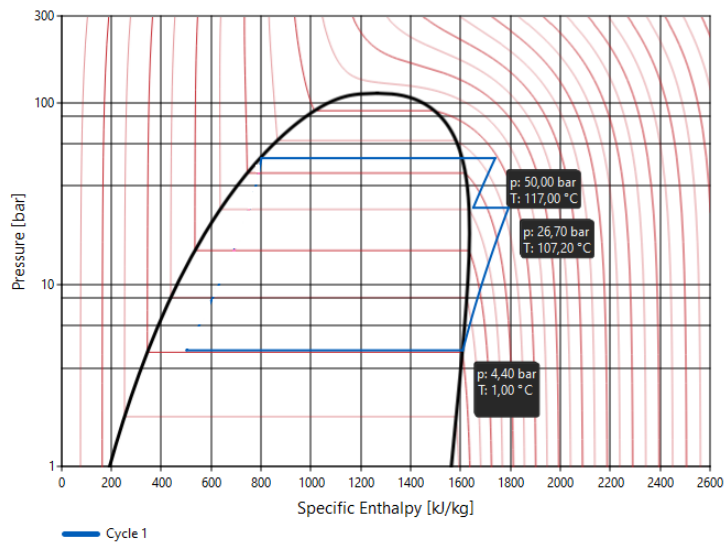


Figure 2: Log Ph diagram of ammonia showing high compressor discharge temperature optimized for heating.

The log Ph diagram also shows how the inter-cooling is vital to keep the gas discharge temperature at a relatively low level.

2.2 Ground Source Heat Pumps using NH₃

In 2018 (Wu et al., 2018) investigated the progress in GSHPs using NFWs. For ammonia there are mainly 3 different cycle types that are relevant, vapor-compression cycles, absorption cycles and hybrid compression-absorption cycles.

For the vapor-compression cycle they investigated several types of heat pumps. In 2008 (Palm, 2008) designed a prototype water to water heating-only heat pump with 9 kW heating capacity. This heat pump was able to heat DHW above the condensing temperature of 48 deg with only 100g of NH₃. With an evaporating temperature ranging from -13 to 2 deg, the heat pump had a measured COP of 3.8-4.8.

In 2017, (Zajacs et al., 2017) designed a NH₃ GSHP with 8.4 kW heating capacity that could provide both DHW and space heating. In this heat pump, they optimized the tank volume to minimize the heating demand during peak hours with high electricity costs. For a T_{evap} of -3°C and T_{cond} of 40°C, they reached a COP of 4.0.

(Jensen et al., 2017) investigated the possibility of connecting two heat pumps in series for a district heating network. The connection was made by connecting the liquid sides of the evaporators in series to enable a large temperature change in the fluid used as a heat source. By extracting geothermal heat at 73°C, it was possible to deliver 7.2 MW heat at a condensing temperature of 85 deg. Different refrigerants was investigated, and NH₃ was found to be the most promising for this use.

When used in cold regions, vapor-compression GSHPs can cause ground thermal imbalance, which will reduce its capacity after years of operation. (Wu et al., 2013) looked at the possibility of using an absorption system instead to avoid this problem. This system had a lower $\text{COP}_{\text{heating}}$, but a higher $\text{COP}_{\text{cooling}}$. By extracting less heat in the winter, and adding more in the summer, the problems with thermal imbalance was drastically reduced. In 2015 (Wu et al., 2015), suggested using a hybrid absorption GSHP with an integrated cooling tower to reduce the number of required boreholes, without increasing the thermal imbalance of the ground. It was found that compared to a conventional electrical GSHP, the number of boreholes and occupied land

area could be reduced by up to 50%. Absorption type GSHPs could be an alternative in cold climates, when heating is the most dominant usage of the heat pump, because it has a relatively low cooling efficiency.

In a hybrid compression-absorption cycle, an alternative is to replace the evaporator and condenser from a vapor-compression cycle with a generator and an absorber (Kim et al., 2010), as shown in the sketch in figure 3. This system has a temperature glide that facilitates for applications with wide temperature variations. (Jensen et al., 2015) This cycle also has the ability of producing hot water with reasonably low pressures. This varies from the vapor-compression cycle, which requires very high pressures to produce hot water (Gudjonsdottir et al., 2017). (Jensen et al., 2017) investigated the possibility of using a hybrid compression-absorption system instead of the vapor-compression system in series, which was presented earlier in this section. They discovered that such a system can be suitable when there is a high temperature requirement and a high heat source temperature.

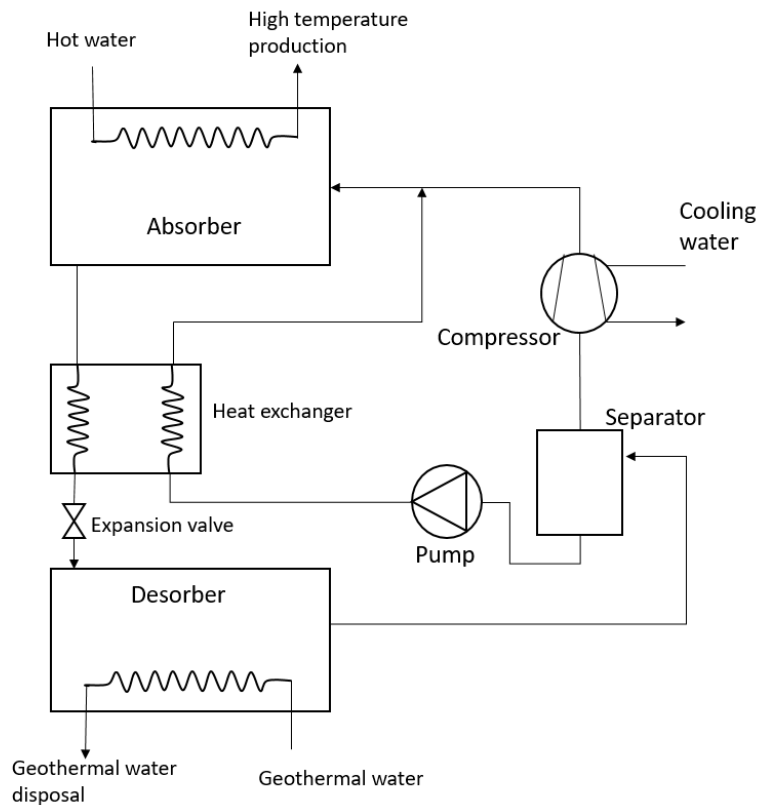


Figure 3: Compression-absorption

Another alternative for a hybrid compression-absorption cycle is to have a compression assisted absorption cycle. This system can increase the absorption pressure, and increase the amount of refrigerant that is absorbed by the absorbent. This was investigated by (Wu et al., 2016), and through experimental comparisons, they found that this technique could lower the generator input from 125°C to 110°C, and increase the heating capacity by 96.4%.

2.3 Small ammonia heat pumps for space and hot tap water heating

In the residential sector, R-410A is the most commonly used refrigerant for heat pumps. However, it is not a long term solution because of its high GWP value of 1725. This has led to exploration of other refrigerants for use in these kinds of heat pumps. During the last 10 years, there have been many attempts to implement ammonia in these systems, but most of them have failed due to a lack of components. It is impossible to use ammonia as a direct substitute for R-410A due to the big difference in pressure and performance. These systems are also often made of copper, which in contact with ammonia will corrode. Therefore specific components to provide long-term operation of an ammonia heat pump is needed.

(Zajacs et al., 2017) have published a report on this specific subject. They gathered previous information about the subject and designed a system to see if it was possible to make a functioning ammonia heat pump for this kind of use.

Simulations of this heat pump showed that this heat pump had a $COP = 3$ with $T_{\text{evap}} = -3^{\circ} \text{C}$ and $T_{\text{cond}} = 40^{\circ} \text{C}$. With this report, Zajacs proved that it is possible to use ammonia not only for large capacity systems, but also for household applications. There are however some disadvantages to the ammonia systems. Because of the high discharge gas temperature, there are limitations when it comes to condensation temperature, which limits its use for high-temperature heating applications. These kinds of heat pumps should also be installed outside of the house due to the toxicity of ammonia.

3 Theory

3.1 Basic principle of the refrigeration cycle

The general refrigeration cycle consists of four parts, a compressor, an expansion valve, a condenser and an evaporator (Eikevik, 2015a). Figure 4 presents a principle sketch of a basic refrigeration system.

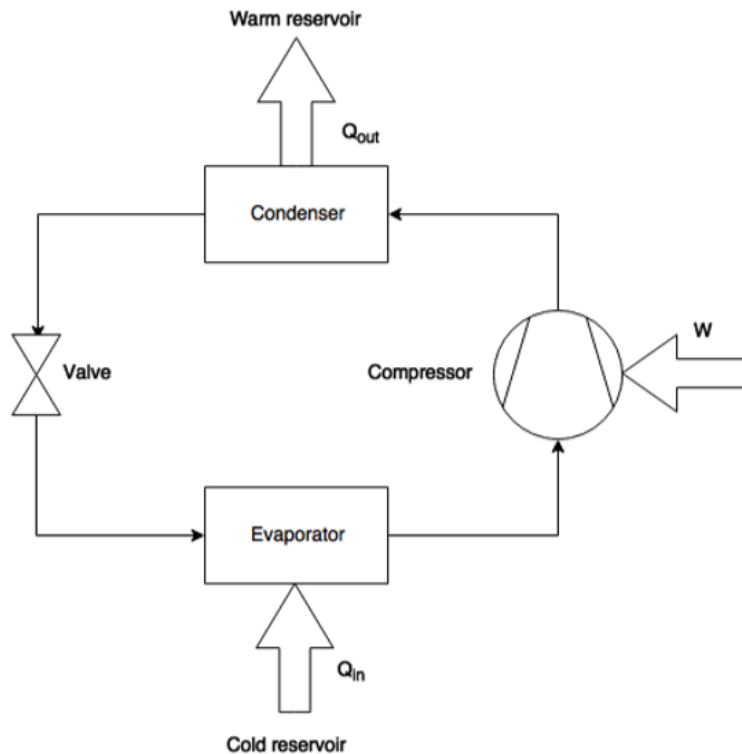


Figure 4: Principle sketch of a refrigeration cycle

The principle of a refrigeration cycle is to extract heat from a heat source, and reject the heat to a higher temperature area, also known as a warm reservoir. To extract heat from the heat source, the refrigerant that flows through the evaporator has to have a lower temperature than the heat source. This forces a heat transfer from the heat source to the refrigerant through evaporation. After the refrigerant is evaporated, it is continuously removed by a compressor. By removing the vapour, the compressor works to maintain a constant pressure in the evaporator. The compressor will also increase the pressure of the vapour to a point where the discharge temperature is higher than that of the warm

reservoir. The compression is the process in the system that consumes work, which is supplied as electrical energy. The energy consumption will vary with different compressors and their isentropic and volumetric efficiencies, as well as the degree of pressure lift through the compressor (Eikevik, 2015a).

After compression, the refrigerant will flow through the condenser. The working fluid will have a higher temperature than the warm reservoir, which will lead to a heat transfer from the working fluid to the reservoir. This process will condense the refrigerant and bring it to a two-phase state. After condensation, an expansion valve will reduce the pressure of the refrigerant by expansion. This leads to a temperature decrease, and increases the liquid fraction of the refrigerant. Lastly, the refrigerant flows through the evaporator, and this continues in a closed cycle (Eikevik, 2015a).

The heat that is rejected from the condenser can be described as the heat absorbed in the evaporator in addition to the work that is done by the compressor. This is shown in equation 1.

$$\dot{Q}_{\text{out}} = \dot{Q}_{\text{in}} + \dot{W}_{\text{comp}} \quad (1)$$

In this simplified system, the only work supplied to the system is to the compressor. However, in a real system, the total work supplied will also consist of electrical work to other components. This total work is needed to find the COP of the system. There are two different types of COP, one for heating and one for cooling. These equations are given as equations 2 and 3 (Bergwitz-Larsen, 2017).

$$COP_{\text{heating}} = \frac{\dot{Q}_{\text{cond}}}{\dot{W}_{\text{total}}} \quad (2)$$

$$COP_{\text{cooling}} = \frac{\dot{Q}_{\text{evap}}}{\dot{W}_{\text{total}}} \quad (3)$$

3.1.1 Isentropic efficiency

In an ideal process, all the work from the compressor shaft would enter the refrigerant, but in reality this is not possible. The isentropic efficiency introduces the losses due to compression. This efficiency is defined as the ratio between the work in an ideal process (isentropic), and the actual work consumed by the compressor (Eikevik, 2015b). Equation 4 is used to calculate the isentropic efficiency, which shows that the actual work consumed by the compressor is higher than the theoretical minimum work. $h_{2, \text{is}}$ is the enthalpy value after compression with isentropic compression, h_2 is the real enthalpy value after compression and h_1 is the enthalpy value before compression.

$$\eta_{\text{is}} = \frac{\dot{W}_{\text{comp, is}}}{\dot{W}_{\text{comp}}} = \frac{\dot{m}_r * (h_{2, \text{is}} - h_1)}{\dot{m}_r * (h_2 - h_1)} = \frac{h_{2, \text{is}} - h_1}{h_2 - h_1} \quad (4)$$

3.1.2 Volumetric efficiency

The volumetric efficiency describes the reduction in volumetric flow through the compressor. Related losses are due to internal leakage between compression chambers, heat and flow losses and expansion of internal gas in the compressor cylinder. Further, the volumetric efficiency is calculated by finding the ratio between the suction volume (\dot{V}_{in}) and stroke volume (\dot{V}_{s}). (Eikevik, 2015b) The suction volume is defined as the volume that is required to be removed from the evaporator in order to achieve the desired refrigeration capacity. The stroke volume is the actual volume that is removed by the compressor. Due to the volumetric losses, the stroke volume is higher than the suction volume. The volumetric efficiency is given by equation 5 (Eikevik, 2015b).

$$\lambda = \frac{\dot{V}_{\text{in}}}{\dot{V}_{\text{s}}} = \frac{\dot{m}_r * \nu_1}{\dot{V}_{\text{s}}} \quad (5)$$

\dot{m}_r in the equation is the mass flow rate of the refrigerant, and ν_1 is the specific volume of the refrigerant at the inlet.

3.2 Ammonia as a working fluid

Ammonia is a long term and environmentally benign working fluid, which neither contributes to ozone depletion nor global warming. This can be seen from the ODP and GWP values, which are explained in chapter 3.2.1, from table ???. It is considered as one of the best refrigerants seen from a thermodynamic and technical view. Because of this, ammonia has been the most frequently used working fluid in industrial applications. It is also considered the most proven among the natural working fluids since it has been used in industrial refrigeration and other large-scale applications for more than a century (Stene, 1998). Because of the relatively low NBP and high critical temperature, ammonia covers a wide range of heat pumping applications, as it can be used for both heat pumps and refrigerating systems. Ammonia however has a low critical temperature compared to several other working fluids, which limits its use for HTHPs (Eikevik, 2015c).

Properties of common natural working fluids							
Ashrae number	Name	ODP	Net GWP 100 year	Molar mass (g mol ⁻¹)	Normal boiling point (°C)	Critical temp (°C)	Critical absolute pressure (kPa)
R-290	Propane	0	3,3	44,1	-42,1	96,7	4248
R-600	Butane	0	4,0	58,1	0,0	152,0	2796
R-600a	Isobutane	0	3,0	58,1	-11,7	134,7	3640
R-601	Pentane	0	4,0	72,1	96,1	196,6	3358
R-717	Ammonia	0	0,0	17,0	-33,3	132,4	11280
R-718	Water	0	0,2	18,0	100,0	373,9	22060
R-744	Carbon dioxide	0	1,0	44,0	-78,0	31,0	7380

Table 1: Comparison on different refrigerants physical properties.

Table 1 shows the properties of common natural fluids (Bamigbetan et al., 2017). As we can see from this table, ammonia has a low molar mass compared to most other NWFs. Ammonia also has an exceptionally high specific enthalpy of evaporation, Δh (kJ/kg). Because of this, the mass flow in ammonia systems will be drastically lower than for other NWFs (Stene, 1998). As shown in equation 4, the compressor work is given as:

$$\dot{W}_{\text{comp}} = \dot{m}_r * (h_2 - h_1) \quad (6)$$

The energy input to the system is therefore very dependent on the mass flow

of the refrigerant.

3.2.1 GWP and ODP

The GWP (Global Warming Potential) of a chemical results from the combination of its radiative forcing and atmospheric lifetime, together with the time frame for evaluation. The radiative forcing is defined as the change in net irradiance at the tropopause due to the change in atmospheric concentration of a trace gas resulting from a pulse release of that gas (McLinden et al., 2014).

The ODP (Ozone Depletion Potential) represents the relative measure of the overall impact that a substance has on the ozone layer. The higher the ODP-value of a compound, the more it will contribute to ozone destruction over the long term (Barbara J. Finlayson-Pitts, 2000). In principle, it is not possible to determine an acceptable value of ODP except for 0. In theory, all compounds with an ODP-value larger than 0 will contribute to destruction of ozone in large enough quantities (Rodriguez, 2007).

3.2.2 Toxicity and flammability

A barrier ammonia has had to overcome is the fact that it is both toxic and flammable, so the safety standards and regulations are very strict. Auto-ignition is as high as 651° C and 15% volume in dry ambient air, so special explosion proof measures are not needed. The smell of ammonia is detectable from 5-50 ppm, and the IDLH concentration is 500 ppm (Stene, 1998). Because of this, reparations can be completed before the concentration reaches dangerous levels.

The high toxicity of ammonia prevents direct use in applications where leakage is considered high risk (Bamigbetan et al., 2017). Because of this; a secondary cycle must be implemented, which reduces the possible outlet temperature in the heat sink.

3.2.3 Corrosion

Ammonia is compatible with steel, stainless steel, iron and aluminium. It will however corrode copper, zinc and copper based alloys. For that reason, it is

only possible to use open compressors in an ammonia heat pump. In hermetic and semi hermetic compressors, the ammonia will come in contact with copper (Stene, 1998).

3.3 Piston compressors

The Piston compressors can be delivered in sizes up to 1500 kW thermal performance at 40 bar for ammonia at $T_{\text{cond}} = 70^{\circ}\text{C}$ and $T_{\text{evap}} = 2^{\circ}\text{C}$ with two-stage compression. The normal pressure level however, is 25 bar. Piston Compressors with a design pressure of 40 bars were introduced in Norway in 1992, and raised the maximal outgoing water temperature to about 70 degrees. This increased its potential for usage in heat pumps (Selvåg, 2007).

Piston compressors can be built for both one-stage and two-stage compression. The most important factor to consider when choosing if the system should use one-stage or two-stage compression is the compression ratio π , which is given as the ratio between P_1 (inlet pressure) and P_2 (outlet pressure). This is shown in equation 7 (Eikevik, 2015b).

$$\pi = \frac{P_2}{P_1} \tag{7}$$

The overall efficiency of the compressor is highly dependent on the pressure ratio. This is shown in figure 5.

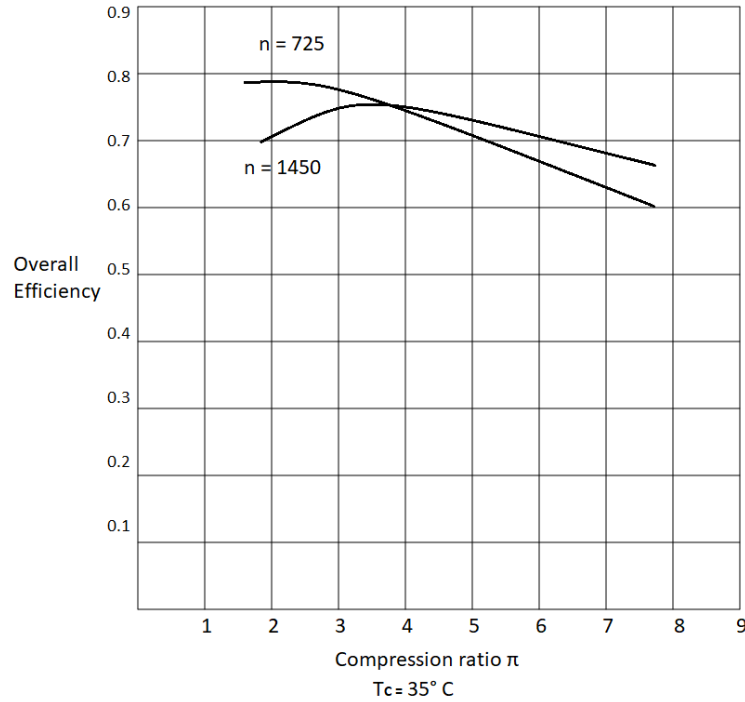


Figure 5: Compressor efficiency at different compression ratios with ammonia as refrigerant with different rotational speed, n (rpm)

As shown in the sketch, the efficiency varies considerably with changing π (C. Koelet and B. Gray, 1992). This can be used to determine if the system should have one-stage or two-stage compression. The SPF also has to be taken into consideration when choosing between the two different solutions. The SPF describes how much heat is delivered from the system compared to the electrical energy input. It is calculated by equation 8 (Kime et al., 2018).

$$SPF = \frac{\text{Total heat energy output per annum (kWh)}}{\text{Total input electricity per annum (kWh)}} \quad (8)$$

By introducing two-stage mode to the compression, the SPF can be lifted by as much as 20-40%. But the investment cost of the compressor will be 80-100% higher compared to a single-stage system (Stene, 2008). Thus, the higher investment cost must be compared to the economical benefit of a more efficient system, which will have lower energy costs.

3.3.1 Part Load

Due to considerable variations in heating and cooling loads and differing temperature requirements in the heat distribution system in buildings, an ammonia heat pump should be designed to have a high efficiency at part load operations. In these systems it is recommended to use reciprocating compressors or inverter controlled screw-compressors with variable volume ratio. Figure 6 shows the compressor efficiency for a 200 kW reciprocating and screw compressor (Stene, 2008).

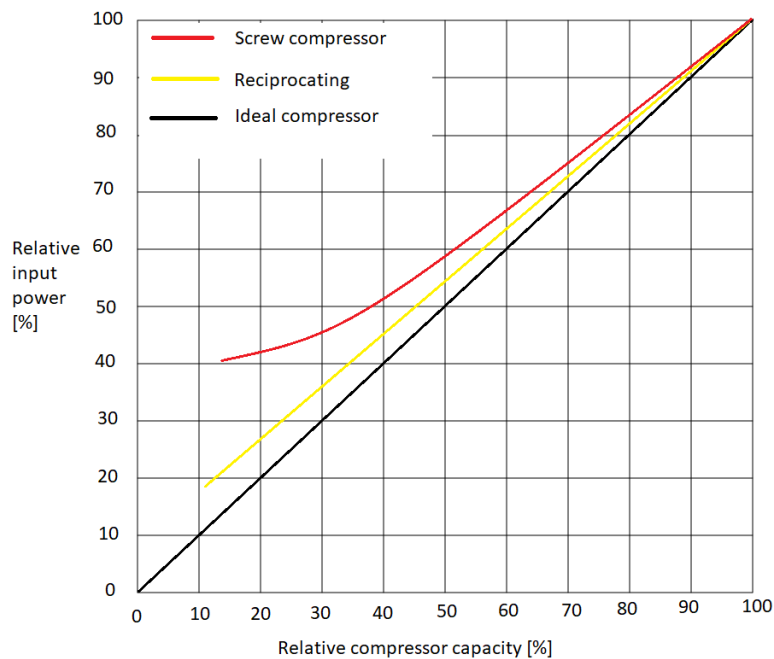


Figure 6: Compressor efficiency at part load

The most common method of capacity control of the compressor to achieve part load is to put one or more cylinders out of action. This is done by a valve-lifting system, which controls the valves on the suction side of the cylinders. This kind of capacity control is called the valve-lifting method. There is however another possibility, which is speed control (C. Koelet and B. Gray, 1992). This method is more efficient, as shown in the sketch in figure 7. However, to be able to use the speed control method, the compressor has to have a variable-speed motor, which increases the investment cost. Speed control is also limited, so it can only reach about 50% reduction in compressor capacity (C. Koelet and B. Gray, 1992).

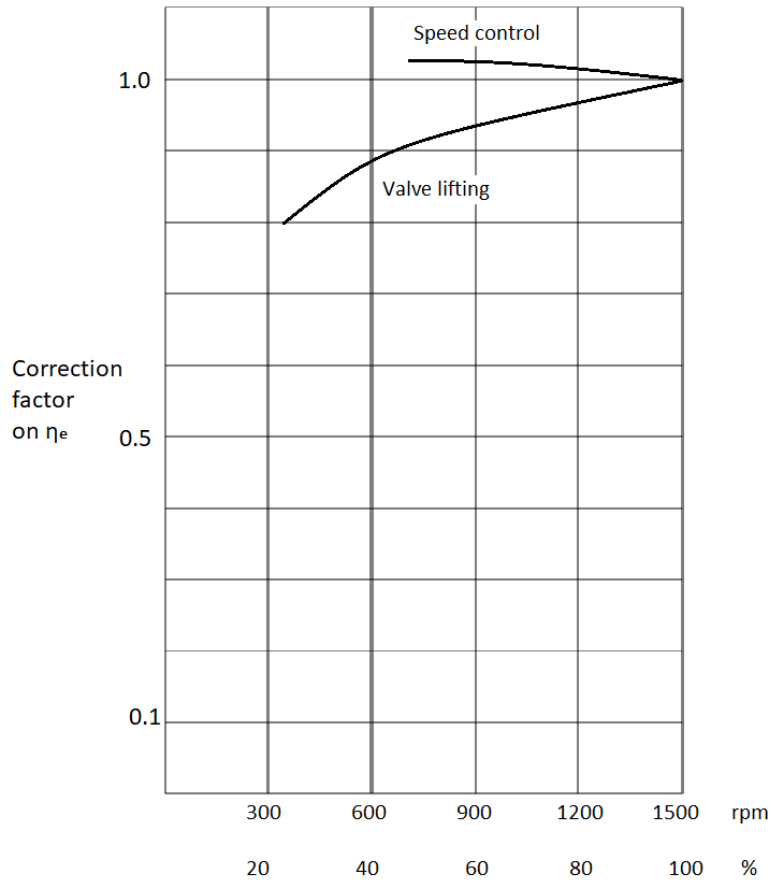


Figure 7: Effects on the power ratio results from different capacity control methods.

3.4 Desuperheater

In two stage compression, introducing a desuperheater between the two stages can significantly increase the efficiency of the system. For ammonia systems, the desuperheater is also important to keep the discharge gas temperature at a lower level. This is shown in figure 8.

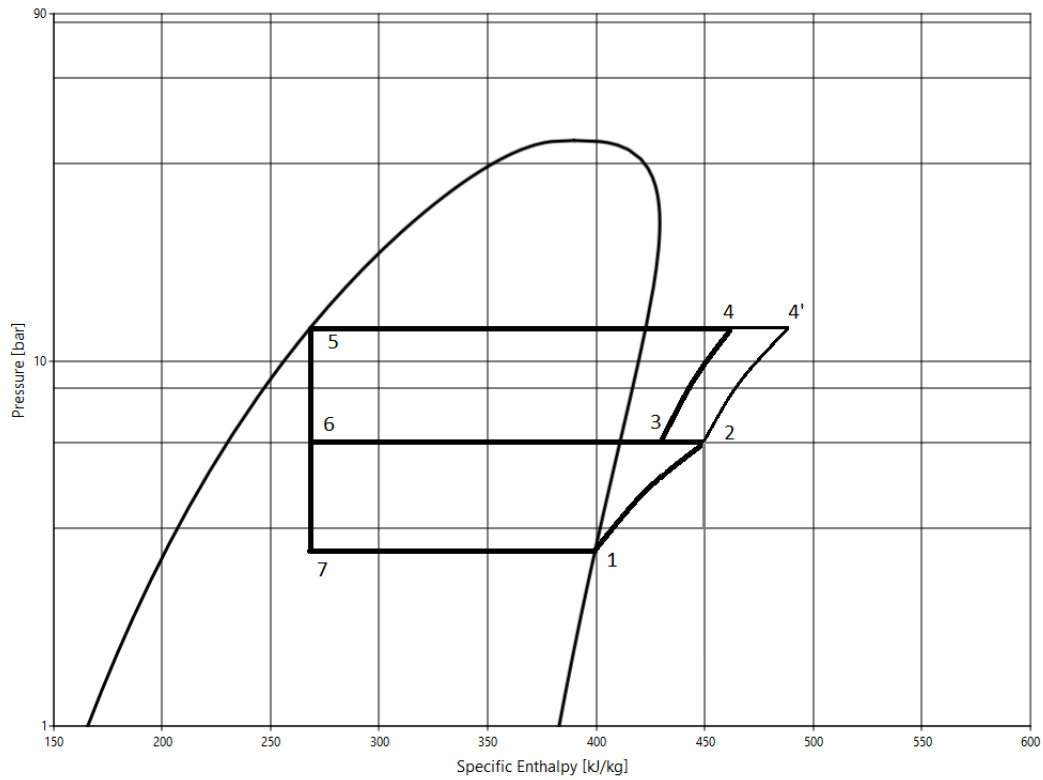


Figure 8: LogP-h diagram of a heat pump with two stage compression and interinjection desuperheating

Here it is shown how implementing a desuperheater will lower the outlet temperature of the discharge gas. Point 4', which shows the second compression stage without desuperheating, is farther to the right in the diagram than point 4, which means that it has a higher enthalpy value, and also a higher temperature. As previously stated, high discharge gas temperatures for ammonia at high pressures limits its use in certain applications. By adding a desuperheater, this limitation is reduced.

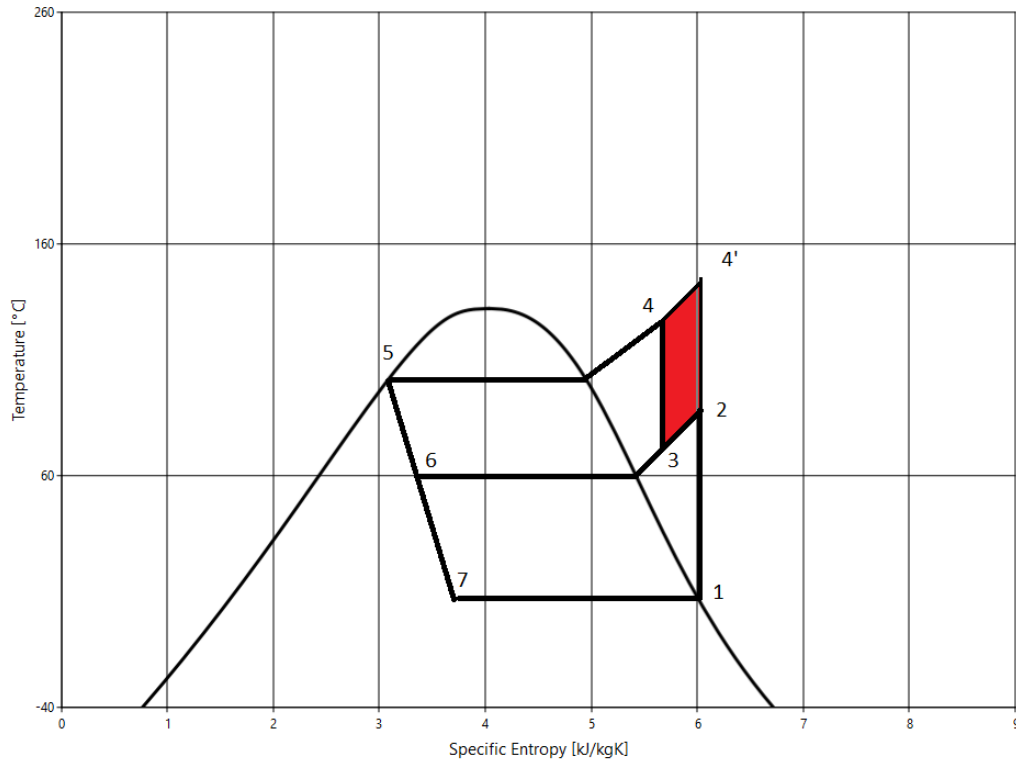


Figure 9: T-s diagram of an ammonia heat pump with two stage compression and inter-injection desuperheating

Figure 9 shows the same cycle in a T-s diagram. In this diagram it is also possible to see the compressor work saved from adding a desuperheater. The coloured part of the diagram represents the work saved from compressing from point 3 to 4 rather than from point 2 to 4'.

3.5 Air cooled Condensers

Air cooled condensers are mainly used to remove latent heat from the refrigerant using air as a coolant. This converts the refrigerant from gaseous to liquid phase. This is a dry direct cooling system where the air surrounding the refrigerant tubes works as the coolant in order to condense the refrigerant (B. Kiran Naik, 2016). The air is passed through the condenser by the use of fans.

There are some downsides to using an air cooled condenser compared to a water cooled condenser. Because of the low heat transfer properties of air, the

heat transfer area has to be larger than that of the water cooled condensers. Because of this, the investment cost and area usage of air cooled condensers are higher than for water cooled condensers. The typical combined investment and operational costs of air cooled condensers are 3.5-5 times higher than for water cooled condensers (John G. Bustamante, 2016).

3.6 Modelica

Modelica is a modeling language which is object oriented. Its main purpose is to simulate natural or man-made systems. The models made in Modelica are equation based with algebraic, differential and discrete equations (Krysander et al., 2018). It can model the dynamic behaviour of technical systems with components from, among others, thermal, electrical and mechanical domains (Martin Otter, 2013).

4 Description of the system

The system installed in GKs offices at Folke Bernadottes Vei 40 in Bergen is a NH_3 reversible heat pump. A principle sketch of the system is shown in figure 10.

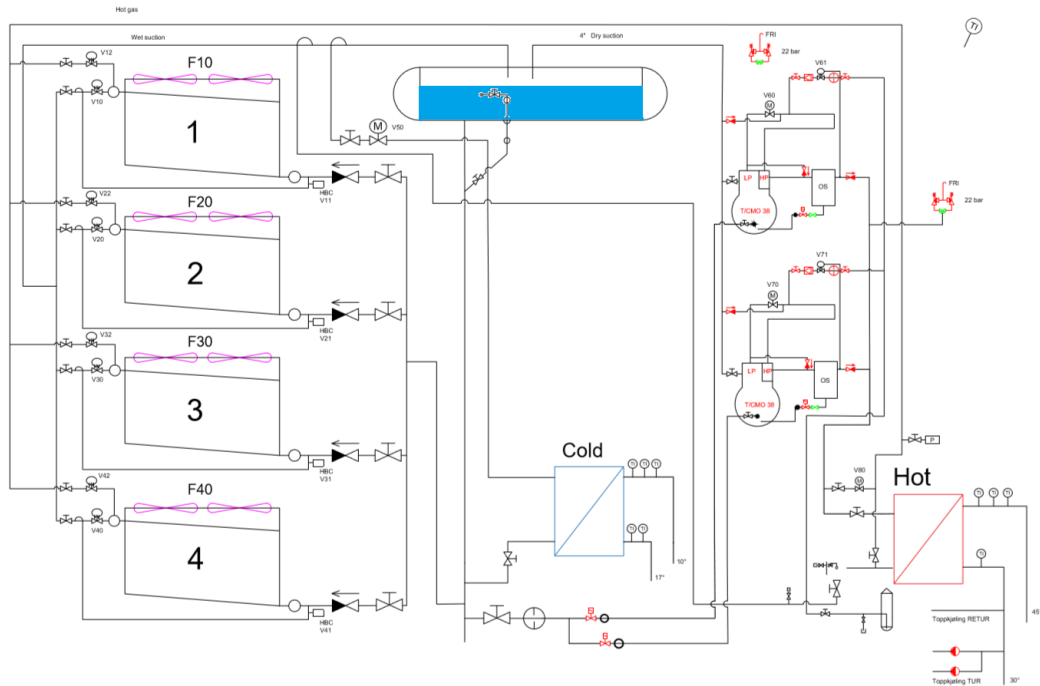


Figure 10: Heat pump system at Folke Bernadottes Vei 40

It can run both single-stage and two-stage compression in each of the two parallel compressors. The heat pump extracts heat from the ambient air in heating mode, and rejects heat to the ambient in cooling mode. The maximum heating demand for the building has been calculated to 250 kW, while the maximum cooling demand is 420 kW. In cooling mode at full load, the design $T_{\text{cond}} 39.4^\circ\text{C}$ while T_{evap} is 7.6°C . In heating mode at full load the design T_{cond} is 46°C , and T_{evap} is -16°C .

As can be seen from the principle sketch, the system can be run in heating, cooling and combined heating and cooling mode. How the system runs is controlled by a system called ClimaCheck. This system measures different values throughout the heat pump and tries to always run it as efficiently as possible. From the ClimaCheck websites, it is also possible to find the results

from all the measurements made. These results have been employed as the basis of comparison with the simulation results from the Modelica models.

To understand how the heat pump is operated, figures 11 and 12 show the stream through the system in the different modes. The arrows show how the refrigerant moves through the different parts of the system.

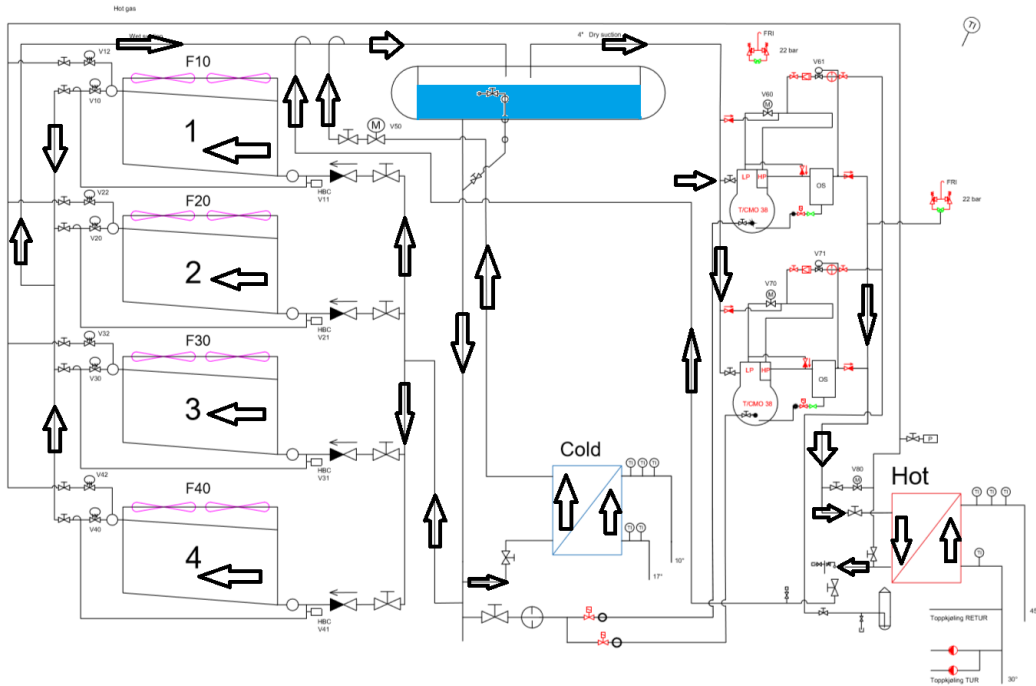


Figure 11: Heat pump in heating mode

For heating operation, the refrigerant is sucked as gas from the receiver and into the two parallel compressors. From here, it goes through the condenser, delivering the heating demand for the building. The refrigerant subsequently goes back towards the receiver, through an expansion valve, lowering the pressure to the receiver pressure level. From the receiver, the refrigerant is also taken as liquid and through the air-heated evaporators, before going back to the receiver. As can be seen in this figure, some of the refrigerant also goes through the water cooled evaporator. This is because there is almost always some cooling demand, so both the air-heated and the water-heated evaporators will be in use.

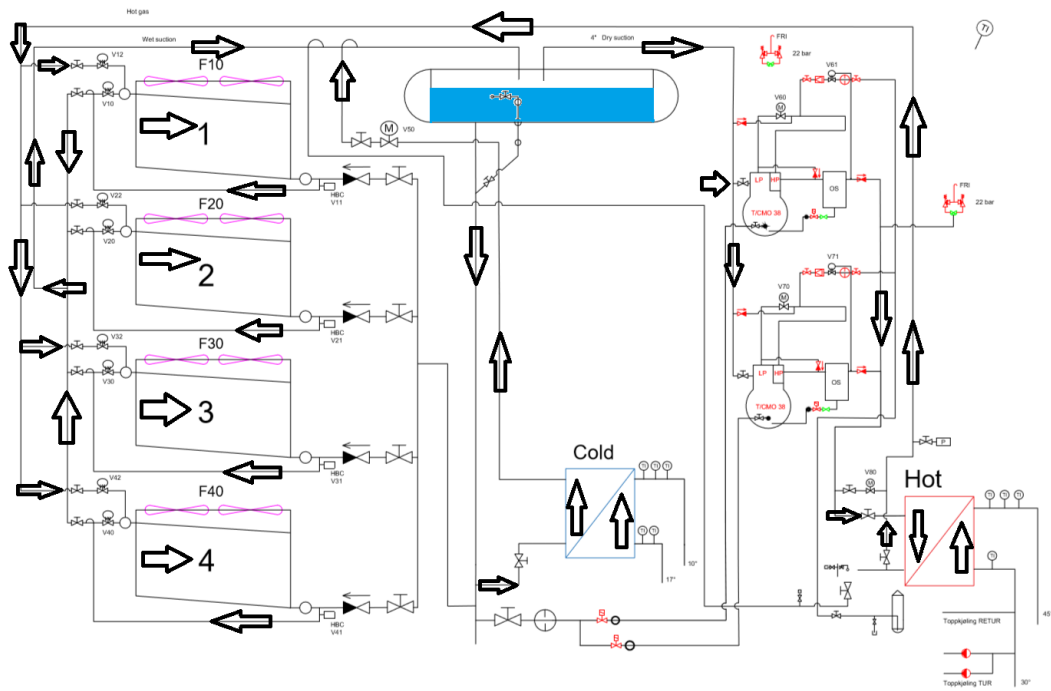


Figure 12: Heat pump in cooling mode

Figure 12 shows the system in cooling operation. The main difference of the two operations is that now, the 4 heat exchangers to the left is used as condensers. The gas will still go through the water-cooled condenser, but from here it will not go back to the receiver. Instead, it goes directly to the 4 air-cooled condensers before going back to the receiver. The evaporator works the same way as in heating mode, but in cooling operation the entire cooling load is being handled in this one evaporator. This mode of operation is also used for de-icing of the air-heated evaporators when necessary.

4.1 Compressors

The two compressors are of the type "Sabroe TCMO 38". These are open Piston compressors with the possibility of two-stage compression within each compressor. They are mostly run in part load operation. The part load operation is achieved by both the valve lifting method and speed control. Cooling of the gas in between the two compressor stages is accomplished by interinjection of refrigerant into the gas stream between the two compressor stages.

The setting of the compressors is to only run two-stage compression when the

outside air temperature goes below -10°C . This temperature setting is possible to change manually.

4.2 Heat exchangers

The evaporator and condenser that delivers the heating and cooling for the building is of the type Alfa Laval M10. The condenser is installed as a counter-flow heat exchanger and delivers heat to a water stream flowing through the condenser. The evaporator is installed with parallel flow. This is because the evaporator is flooded. Having parallel flow is common in flooded evaporators, and by having the warm flow coming in at the bottom, it is easier to keep the boiling going. More technical data for the heat exchangers is given in the appendix.

The four heat exchangers at the left side of figure 10 uses air as the secondary media, in addition to ammonia as the working fluid. They can be run as both air cooled condensers and air heated evaporators. In heating mode they work as evaporators, and in cooling mode they work as condensers.

5 Model

In order to evaluate the heat pump system studied in this report, a model of the system had to be made. This model was designed in the simulation program Modelica. There are certain limitations with this program, mainly that when the model has many components, the system becomes unstable. This is because changing a single value in one of the components affects the whole system, which makes simulations with different conditions problematic. This model is still considered to serve the purpose of this assignment however, because the limitations can be remedied by constructing several models for both single-stage and two-stage compression, using fewer components in each model. This method has the added advantage that less components in a model often gives a more stable system that can provide clearer results. Because of these factors, this is considered a productive model of evaluation for the heat pump system studied in this report. 4 different models were made to describe the system for both single-stage and two-stage compression for cooling and heating of the building.

In the real system, there are several safety valves and backstop valves. These have also been neglected in the model. Since it is a simplified model, only the most pertinent components have been included. The pressure losses through the pipes and heat exchangers have also been neglected.

The model of the heat pump in single-stage heating mode is shown in figure 13, and in single-stage cooling mode in figure 14.

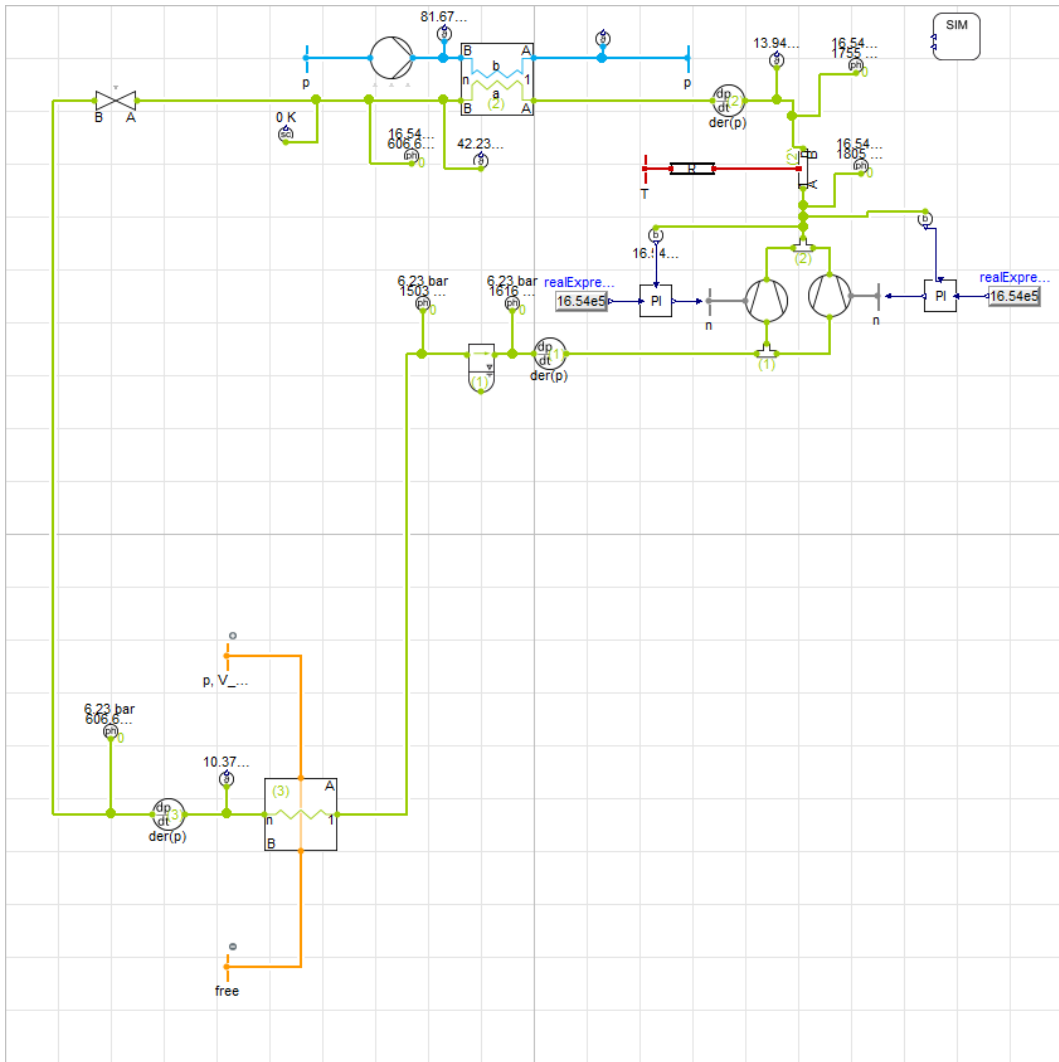


Figure 13: Model of the heat pump in single-stage heating mode

The model works by introducing ammonia in the liquid separator in the middle of the figures. From the liquid separator, NH_3 gas is being sucked into the compressor, thereby keeping the low pressure in the liquid separator. The compressors are equipped with a PI-controller, which measures the pressure just after the compressors. The PI-controller then adjusts the speed of the compressor to obtain the desired high pressure in the condenser. The mass flow through the two parallel compressors are equal.

The pressure after the valve is decided by a pressure state point. This makes sure that the evaporator has the desired pressure. The condenser and evaporator is designed to be as close to the actual heat exchangers in the real system as possible, though some changes had to be made to get the same effect from

the heat exchangers as in the actual system. In the model, the cross flow heat exchangers are modelled with air as the secondary working media. The orange lines in the model is the air flowing through the heat exchangers. The blue lines in the model is the water flow through the condenser and evaporator in each of the two models. The water flow is controlled by a pump, which is set to have the same mass flow as the real heat pump at different conditions.

The pipe between the compressors and the condenser is placed to simulate the heat loss from the compressors. Connected to the pipe is a heat resistor which is connected to the ambient temperature around the heat pump. Through this it is possible to get more similar results to the real heat pump, as it has a significant heat loss from the compressors.

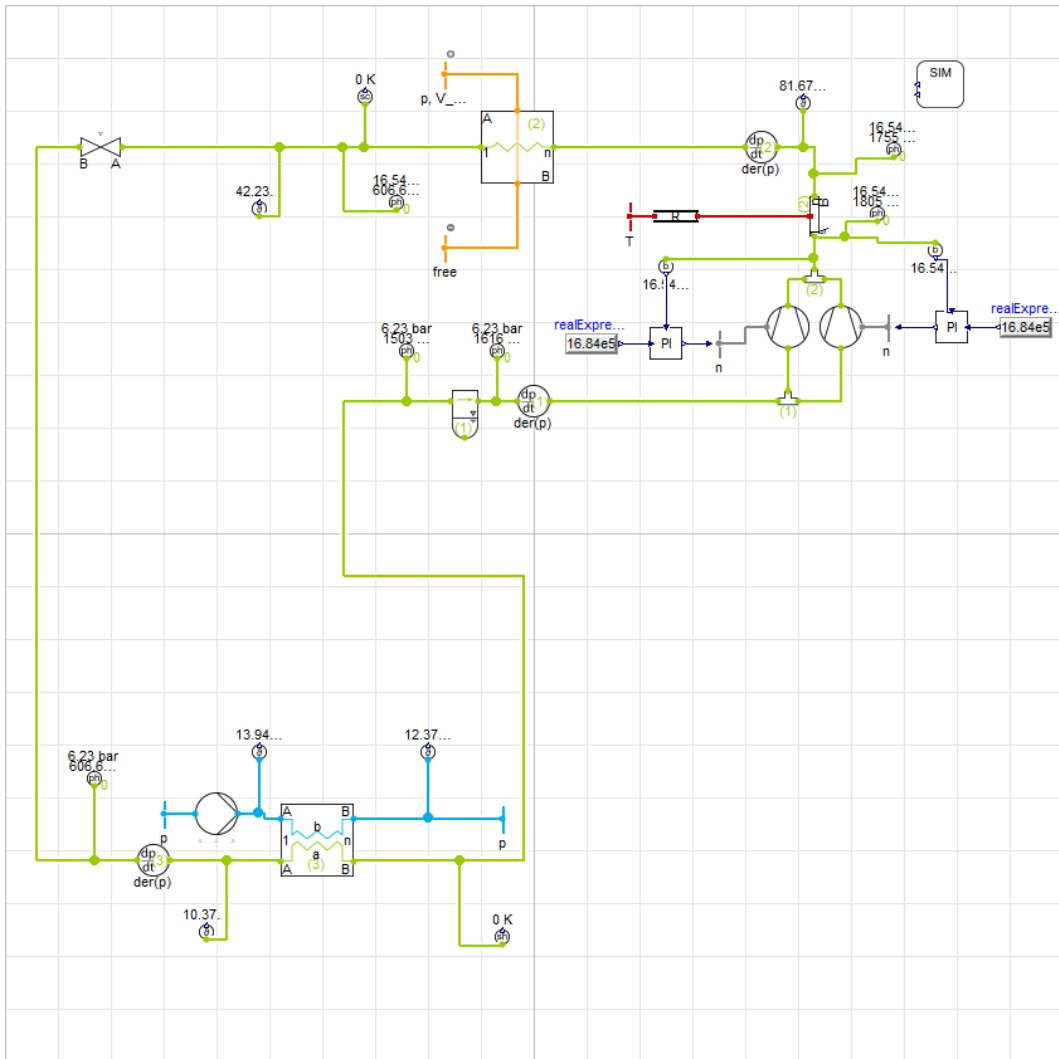


Figure 14: Model of the heat pump in single-stage cooling mode

As can be seen from figure 14, the system works exactly the same way as in the heating mode operations, except for the fact that the condenser now has air as the second media and the evaporator has water. This is to simulate the heat pump in cooling mode. However, the real system is a combination of the two models, with the cross flow heat exchangers as either condensers or evaporators. As mentioned earlier, to do this in the simulation program was not possible.

Following is the models of the system with two-stage compression. The heat exchangers are the same as in the single-stage models, with one exception. A desuperheater is included between the two compressor stages. This has the same water stream as the condenser, so the outlet temperature of the water after the desuperheater is the same as the inlet water temperature of the condenser. This is not the same as the solution used in the real heat pump, which has interinjection of the gas in between the compressor stages. This however did not work in the simulations, so a desuperheater was used instead to get similar results.

Figure 15 shows the model in two-stage heating mode. Here, there are two compressor stages that are controlled by PI-controllers. The controllers measure the pressure right after the compressors, and adjust the speed of the compressors to obtain the desired pressure. There is also two pipes in this model to simulate the heat loss from the compressors. They work exactly the same way as in the single-stage models, but are divided into two separate pipes to get heat loss from both the compressor stages, and not only the last stage.

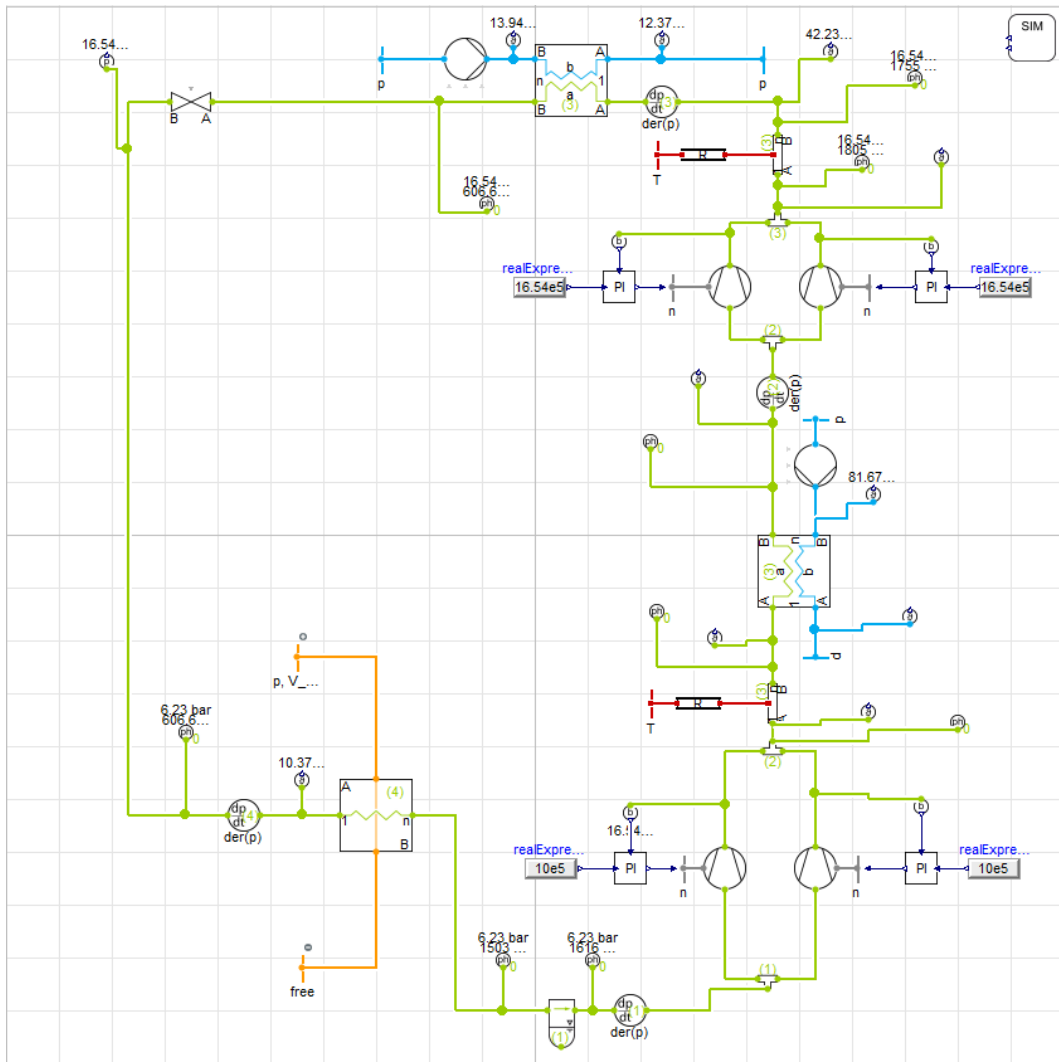


Figure 15: Model of the heat pump in two-stage heating mode

Figure 16 shows the model of the system in two-stage cooling mode. The only difference between this and the two-stage heating model is the heat exchangers. The condenser now has air as the secondary fluid, and the evaporator has water as the secondary fluid, thus delivering the cooling demand to the building.

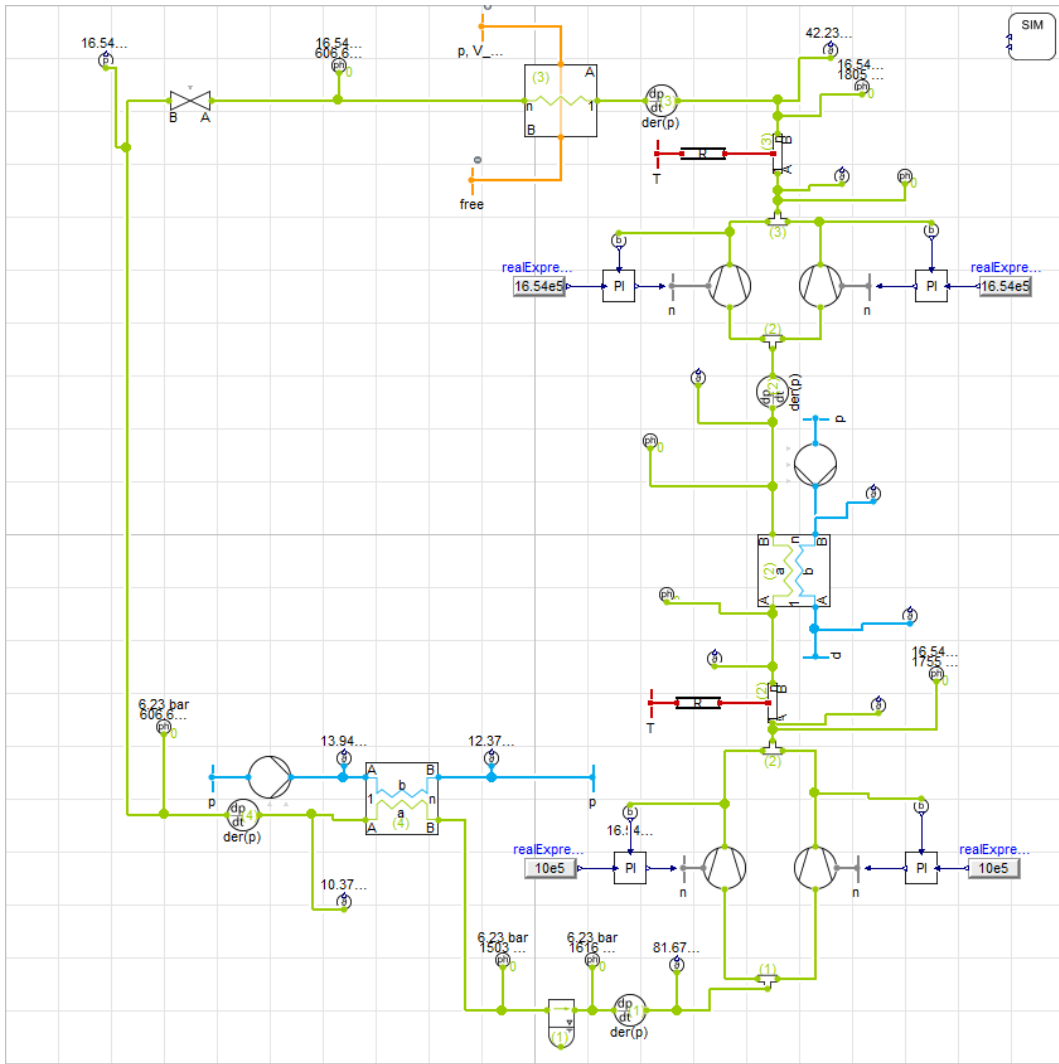


Figure 16: Model of the heat pump in two-stage cooling mode

6 Results

For the results in this section, the simulation has been run with one hour continuous operation. At start-up, the model does not have any ammonia in the different components, except for the liquid separator. For this reason, the results from the first few minutes of operation will not be relevant. In the real heat pump, the refrigerant will be in the different components at all times, including when the heat pump is not running. This will give more stable results, also at start-up. Because of this, the focus will be on the values when approximately steady state is reached.

To get results which is comparable to the actual heat pump, data from different times has been collected from ClimaCheck. Through examining data from different days with different outside temperatures, two days in particular has been chosen to use as a basis for comparison. The two days chosen were among the warmest and coldest in Bergen this spring.

6.1 16th of May 2019

The 16th of May was a warm day in Bergen, with outside temperatures of 24 degrees. Data for this day has been collected from Climacheck. The focus has been on the hour from 12pm to 1pm. Following is a figure which shows some of the values collected from this day. Some excel sheets have also been collected with more exact values in short time intervals between each measurement. From these values an average value for a time period has been calculated. This is to get more stable results for comparison. The excel sheets with the values used can be found in the appendix.

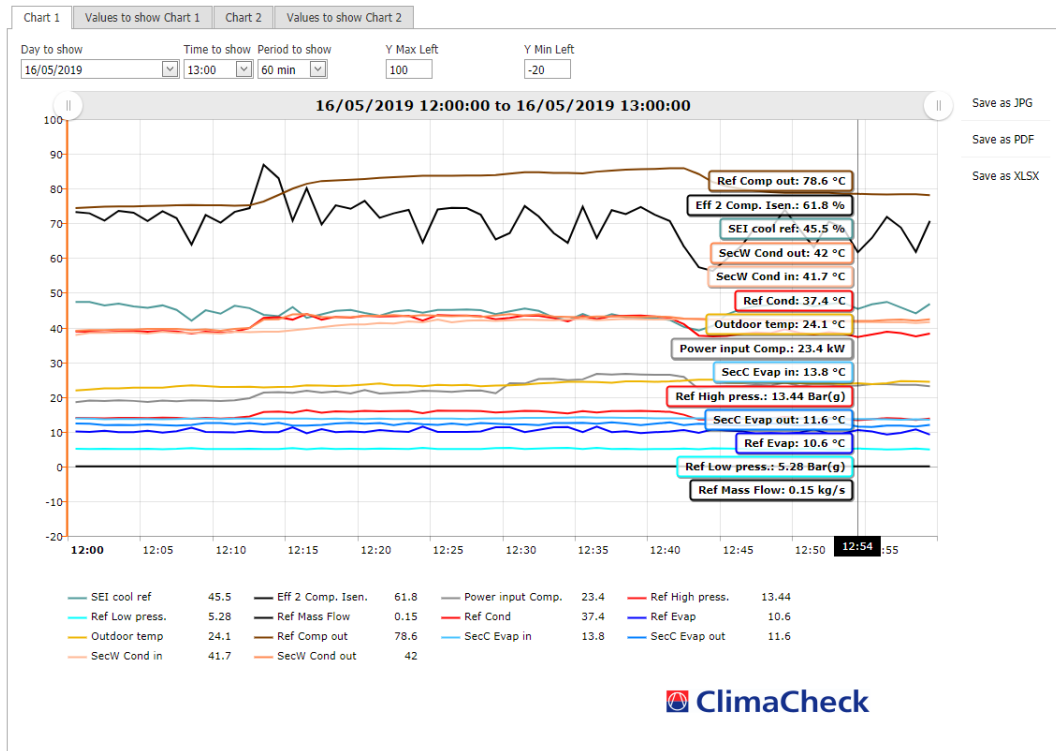


Figure 17: Some values from ClimaCheck for the 16th of May

The design pressures for this day is a low absolute pressure of 6.24 bar and a high pressure of 16.54 bar. This gives an evaporation temperature of 10.44°C, and a condensing temperature of 42.22°C. The cooling capacity found from the ClimaCheck results is 124.48 kW and the heating capacity is found to be 139.81 kW. The compressor is in single-stage mode, and has an isentropic efficiency of 72.6%, and the average work of the compressors is 22.28 kW. This was the main results that was focused on recreating in the model.

6.1.1 Heating

Firstly, the model has to be set to have the same refrigerant mass flow rate as in the results from ClimaCheck. This is important to get similar results for the compressors and the heat exchangers. The average refrigerant mass flow rate was found to be 0.1405 kg/s.

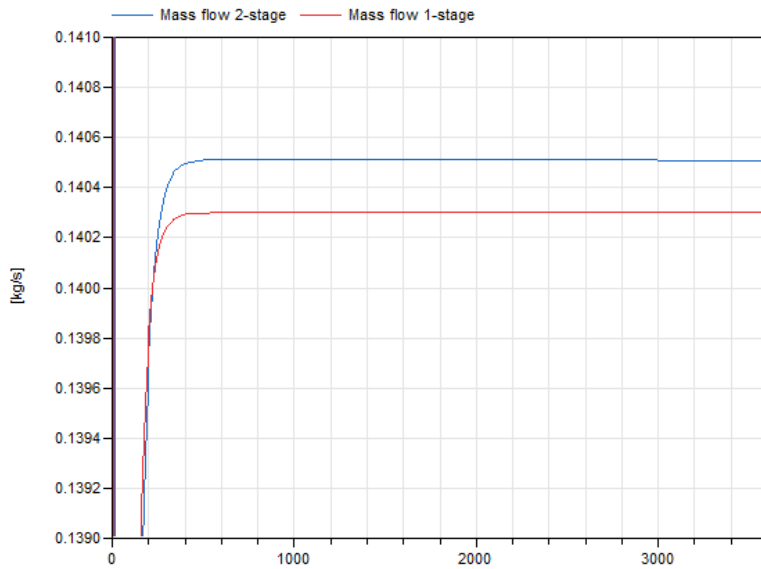


Figure 18: Mass flow of refrigerant through the condenser with single-stage and two-stage compression

The mass flow rate for the single-stage compression simulation ended up being: $m_{\text{flow}} = 0.1403 \text{ kg/s}$. This is not exactly the same as found in ClimaCheck, but a 0.14 % difference is not so high as to effect the results significantly.

For the two-stage compression simulation, the mass flow rate was found to be: $m_{\text{flow}} = 0.1405 \text{ kg/s}$. Here it is exactly the same as in the results for the real heat pump. In figure 18 the results for the mass flow rate in the simulations is shown.

For the given time interval on the 16th of May, the average heat delivery from the condenser for the real heat pump is found to be 139.81 kW. The condenser in the model has been given input values to come as close to this value as possible.

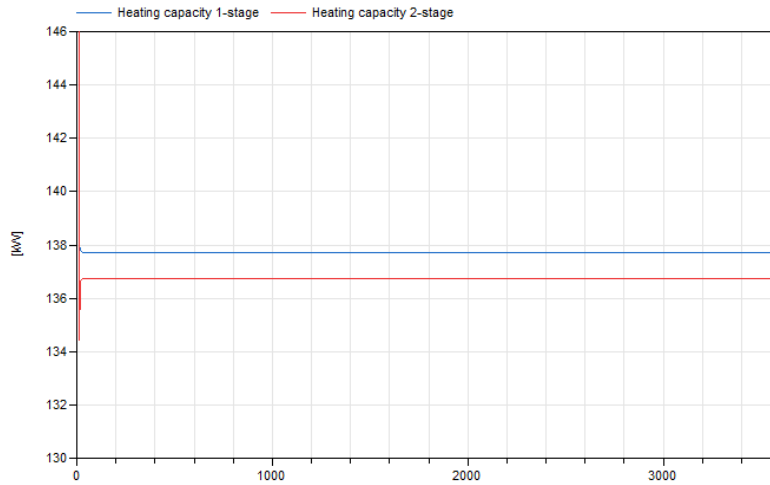


Figure 19: Heating capacity of the heat pump with single-stage and two-stage compression

For the single-stage compression mode, the heat load from the simulation was found to be $Q = 137.73$ kW. This is not as high as in the real system, but within a margin of error that is acceptable. For the two-stage compression mode, the heat delivery from the simulation was found to be $Q = 136.72$ kW. Since the desuperheater will also affect the heat delivered from the system, this must be included in the total heat delivered. This was found to be 0.41 kW, therefore the total heat load from the 2-stage simulation is 137.13 kW. This is shown in figure 19, however without the desuperheater included. This is to better see the differential between the heat exchanger in single-stage and two-stage mode.

The results for the work performed by the compressors is shown in figure 20. This graph shows one of the parallel compressors for both single-stage and two-stage compression. Since the model is designed to have the same work for both of the parallel compressors, the actual work will be double of what is shown in the graph. The compressors in single-stage mode has an isentropic efficiency of 72.6%, as found in the results from ClimaCheck.

For two-stage compression, the isentropic efficiency had to be calculated, since there is no results from ClimaCheck in which to find it. This was accomplished by a VBA code in Excel. This code took into account evaporation temperature, condensing temperature, maximum rpm, minimum rpm, total cylinders, active cylinders and the load. This calculation gave an approximate value for both the isentropic and volumetric efficiency of the compressors. These values where

found to be $\eta_{\text{is}} = 79.8 \%$ and $\lambda = 88 \%$. The code used to find these values was made by Gert Nielsen, and is for that reason not included in the report. Any requests to view this code has to be directed to him. (Nielsen)

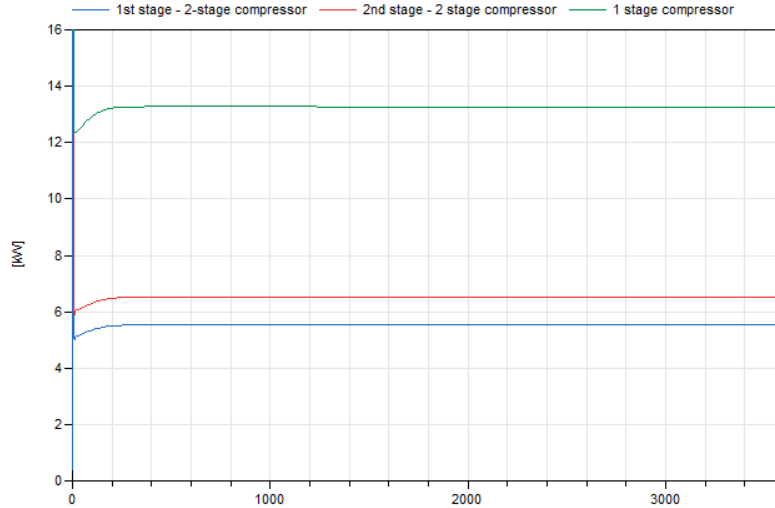


Figure 20: Compressor work in single-stage and two-stage mode

The single-stage compressor work is found to be $2 \cdot 13.28 = 26.56$ kW. The two-stage compressor is divided into two parts: The first stage that lifts the ammonia to the intermediate pressure, and the second state, which lifts it up to the high pressure. For the two-stage compressor, the work was found to be 5.53 kW for the first stage and 6.51 kW for the second stage. In total, the work of the compressors was $(5.53 + 6.51) \cdot 2 = 24.08$ kW.

Following is the log Ph-diagrams for both the heating and cooling mode of the heat pump for the 16th of May. This gives a graphic overview of the system.

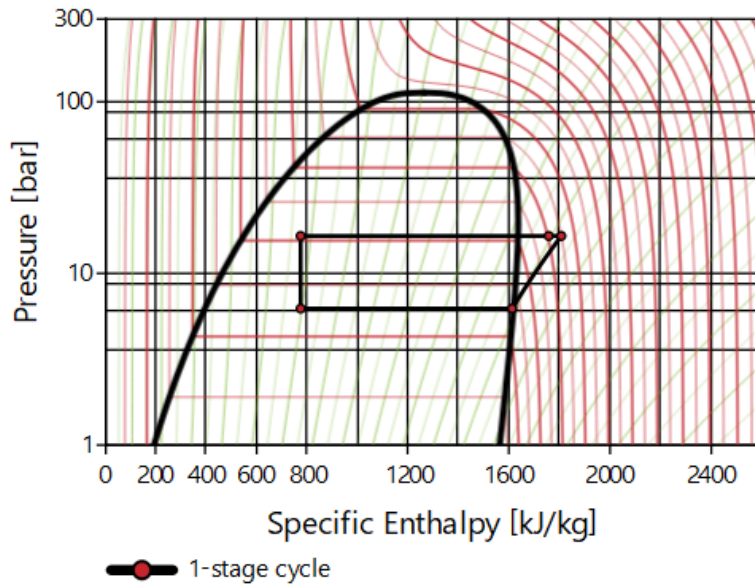


Figure 21: Log Ph diagram of the single-stage cycle

For the 1-stage cycle, the top right point is the state point after the compressors. The point slightly to the left of this point is when the heat loss of the compressor is taken into account.

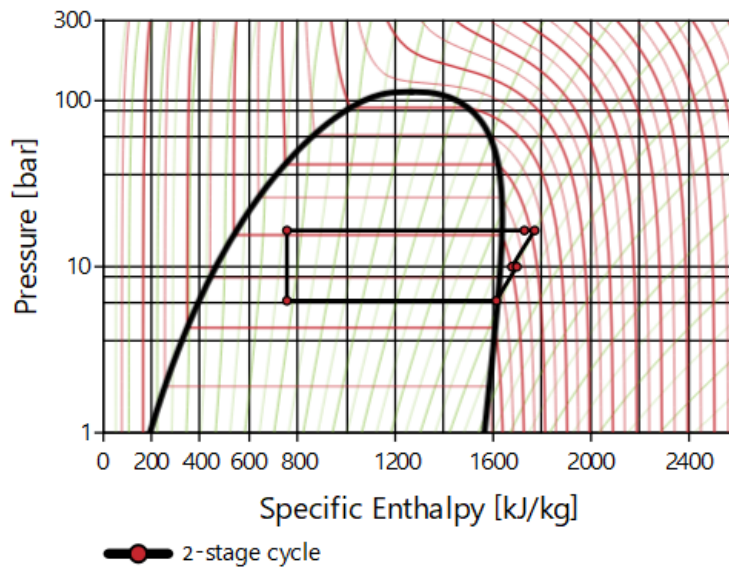


Figure 22: Log Ph diagram of the two-stage cycle

For the two-stage cycle, the de-superheater cools down the gas slightly at an

intermediate pressure of 10 bar. The heat loss from the compressor is also taken into account in this figure, both in the first compressor stage and in the second compressor stage.

From the information gathered through the simulations, the overall efficiency of the system, the COP, can be found.

$$COP_{\text{heating single-stg}} = \frac{\dot{Q}_{\text{cond}}}{\dot{W}_{\text{comp}}} = \frac{137.73kW}{26.56kW} = 5.19 \quad (9)$$

$$COP_{\text{heating two-stg}} = \frac{\dot{Q}_{\text{cond}}}{\dot{W}_{\text{comp}}} = \frac{(136.72 + 0.41)kW}{24.08kW} = 5.69 \quad (10)$$

As seen from these calculations, the system has a 9.6 % higher efficiency when running two-stage compression than single-stage compression.

6.1.2 Cooling

For this part, the results are produced from the model that simulates the cooling mode of the heat pump. Since both the heating and cooling demand of the heat pump is delivered simultaneously from the real heat pump, the refrigerant mass flow and the pressures of the system is equal to the system in heating mode. The average cooling load for the time frame was found to be 124.48 kW.

The mass flow for the single-stage compression simulation was found to be 0.1401 kg/s, as shown in figure 23. It is slightly lower than what was found from the ClimaCheck results, which was 0.1405 kg/s.

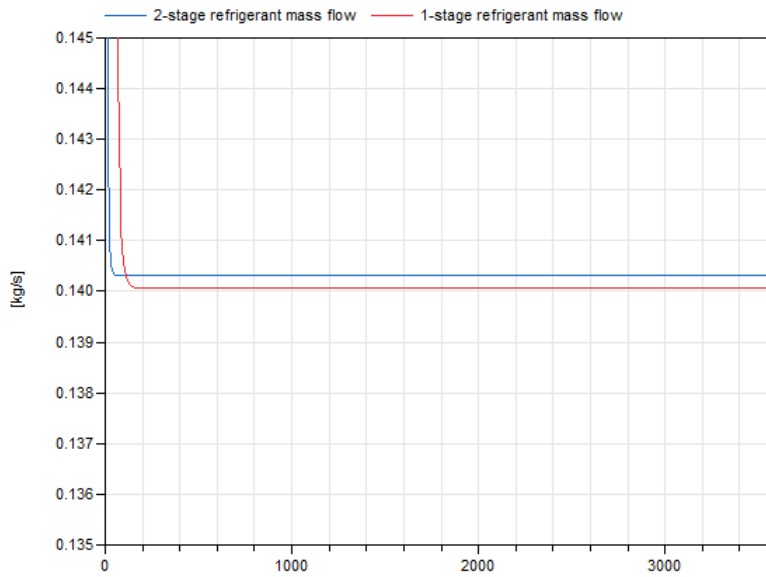


Figure 23: Mass flow of refrigerant through the evaporator with single-stage and two-stage compression

For the two-stage compression simulation, the mass flow of the refrigerant was found to be 0.1403 kg/s. This is closer to the desired value, and close enough to the single-stage mass flow to get comparable results.

From the simulations, the cooling delivered from the water cooled evaporator for single-stage compression is found to be 125.43 kW. This is slightly higher than for the actual heat pump, by a margin of 0.95 kW. As seen from figure 24, the delivered cooling load does not reach steady state, but rather rises slowly from 124 kW to 125.43 after 1 hour operation. Because the increase is so slow, and the heat pump never runs for continuous operation for a long time period, this is not important. Since all the other values has been found from when the simulation has been going for 1 hour, that is the value that is being used for this as well.

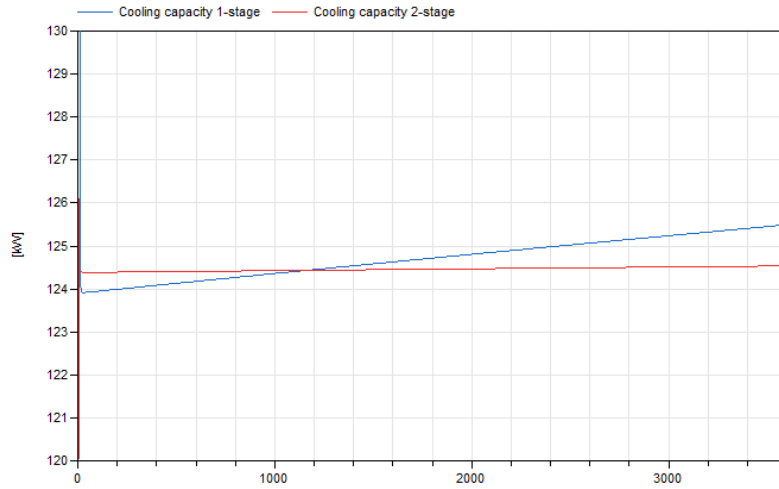


Figure 24: Cooling capacity of the heat pump with single-stage and two-stage compression

For the two-stage compression simulation, the cooling delivered from the evaporator was found to be 124.53 kW. This value is nearly identical to the actual average delivered cooling for the time frame investigated in this simulation.

As can be derived from figure 25, the compressor work for the cooling operation is identical to heating operation. This is important, because the heating and cooling delivered in the real system happens simultaneously in the real heat pump. Therefore, the compressors need to have the same work for the simulations to properly describe the system. The compressor work for single stage compression is 26.56 kW, and for two-stage compression it is 24.08 kW.

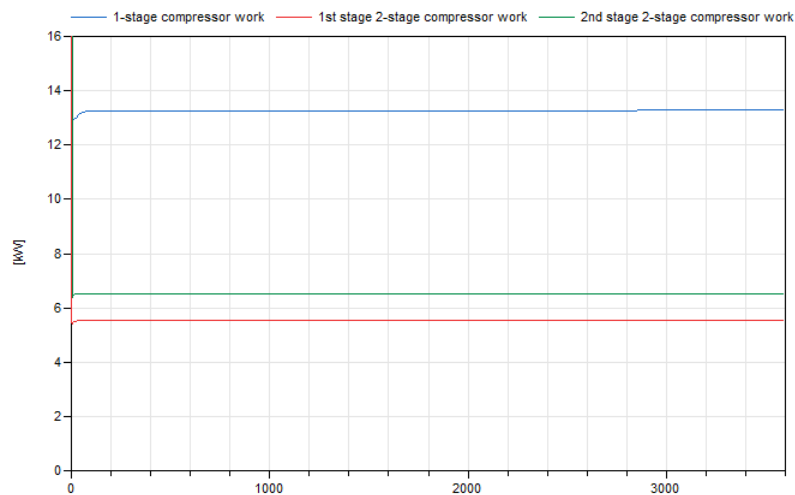


Figure 25: Compressor work in single-stage and two-stage mode

Following, in figure 26 and 27, is the log Ph diagrams for the cooling simulations for single-stage and two-stage compression. The reason for the lower enthalpy values after the condenser compared to the heating mode is that the air temperature is lower than the water temperature through the condenser in heating operation.

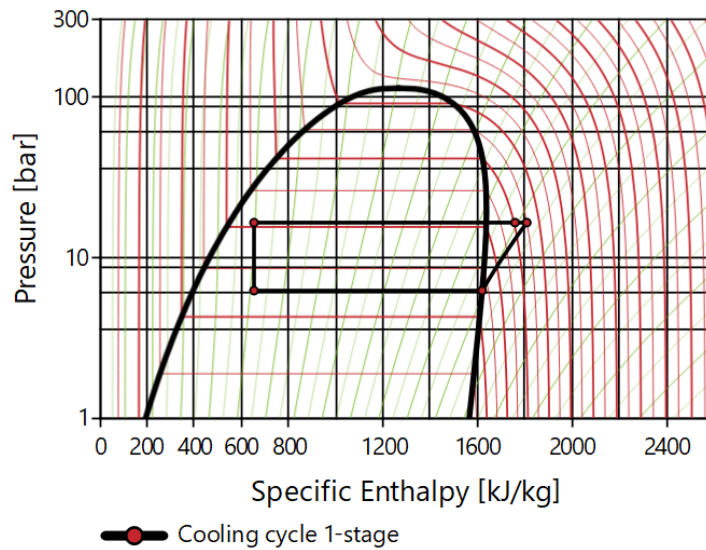


Figure 26: Log Ph diagram of the single-stage cycle

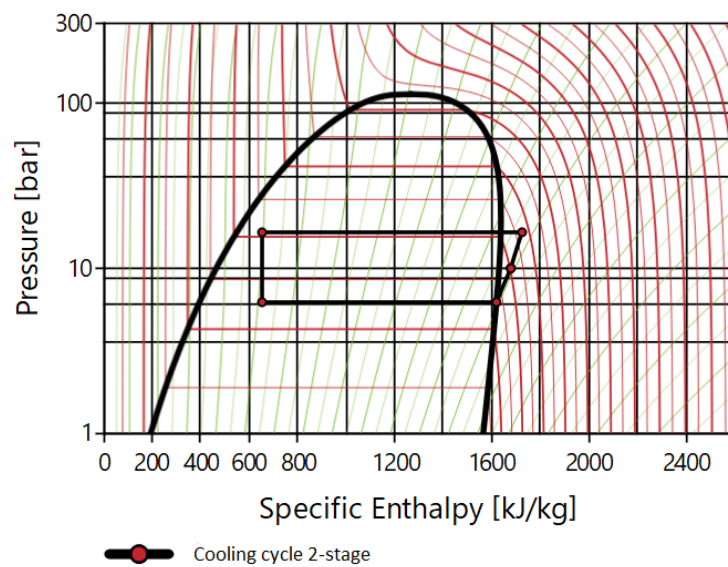


Figure 27: Log Ph diagram of the two-stage cycle

From the values found, the COP for the cooling operation can be calculated, as shown in equation 11 and 12.

$$COP_{\text{cooling single-stg}} = \frac{\dot{Q}_{\text{evap}}}{\dot{W}_{\text{comp}}} = \frac{125.43kW}{26.56kW} = 4.72 \quad (11)$$

$$COP_{\text{cooling two-stg}} = \frac{\dot{Q}_{\text{evap}}}{\dot{W}_{\text{comp}}} = \frac{124.53kW}{24.08kW} = 5.17 \quad (12)$$

The overall efficiency of the heat pump in cooling mode is higher for two-stage compression than for single-stage compression. Two-stage compression has a 9.5 % higher efficiency than single-stage compression with these conditions.

The overall performance of the system in single-stage heat mode is shown as a bar graph in figure 28. This is to better visualize how the heat pump performs under these conditions.

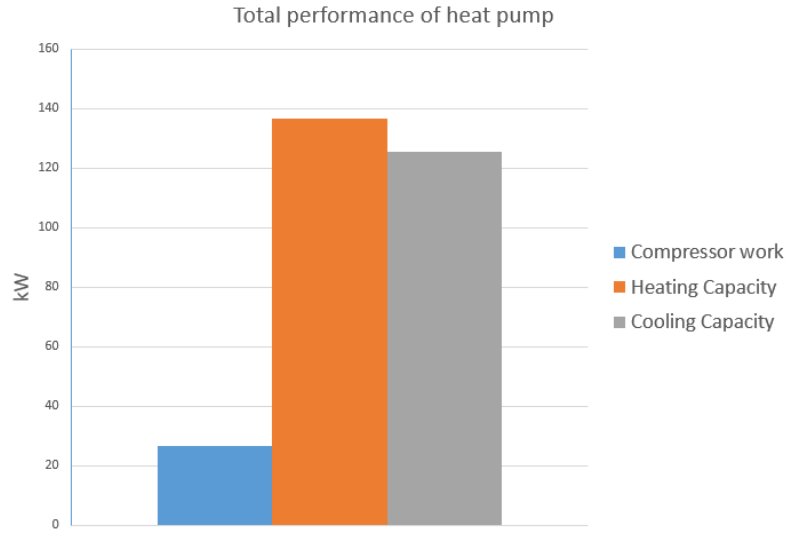


Figure 28: Average delivered heating and cooling compared to the compressor work

6.2 28th of January 2019

The 28th of January 2019 was a very cold day in Bergen. For the time period chosen, from 04:58 AM to 05:47 AM, the average outside temperature was -5.71°C . Because of the time, when there was little activity in the building, the heating and cooling demand was low. The reason for still choosing this time

frame was that the heat pump had stable operation for a long time, which makes comparison with the simulated results easier.

The design pressures for this day was a low absolute pressure of 3.08 bar and a high pressure of 16.84 bar. This gives an evaporation temperature of -8.55°C , and a condensing temperature of 42.90°C . The cooling capacity found from the ClimaCheck results was 72.22 kW and the heating capacity was found to be 85.47 kW. The compressor was in single-stage mode, and had an isentropic efficiency of 66.68%, and the average work of the compressors was 21.83 kW. Many of these values are lower than for the 16th of May, even though the compressor pressure ratio is higher. The main reason for this is that the average refrigerant mass flow through the heat pump was lower than what was the case the 16th of May. For this time frame, the refrigerant mass flow of the system was found to be 0.084 kg/s.

6.2.1 Heating mode

The mass flow for the single-stage compression simulation was found to be 0.084 kg/s. It is equal to the desired value found from the ClimaCheck results. For the two-stage compression simulation, the mass flow was found to be 0.085 kg/s.

The heating load delivered from the condenser in single-stage simulation was found to be 85.15 kW. This value is 0.32 kW lower than what was found from ClimaCheck. For the two-stage simulation, the heat delivered from the condenser is found to be 80.01 kW. These values are shown in figure 29. For the two-stage simulation, there is also some heat delivered from the desuperheater. This value is 2.76 kW, which gives a total heat delivery of 82.77 kW.

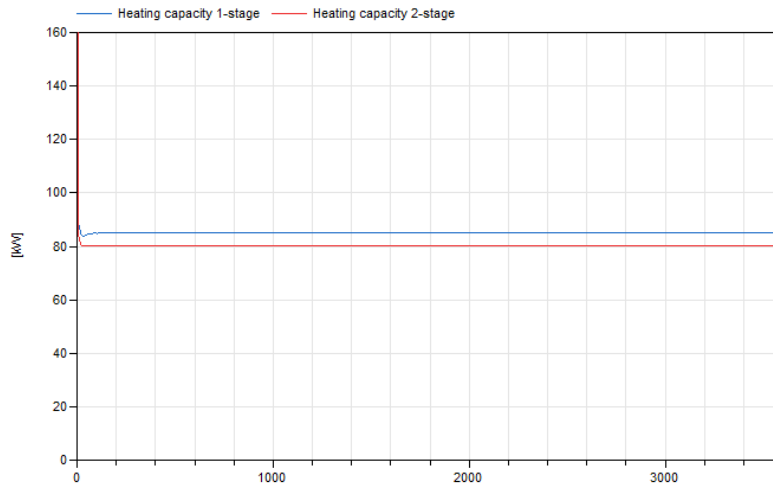


Figure 29: Heating capacity of the heat pump with single-stage and two-stage compression

The compressor work for the single-stage simulation was found to be 15.91 kW for both the parallel compressors, which gives an average compressor work of 31.82 kW. Here, the compressors had an isentropic efficiency of 66.68%, as was the case for the real system. For the two-stage simulation, the isentropic efficiency was found through the VBA Excel code, which gave a result of $\eta_{is} = 74\%$. With this efficiency, the first stage compression work for each of the two compressors was 7.22 kW, while the second stage compression work was 6.32 kW. In total, this gives a compression work of 27.08 kW.

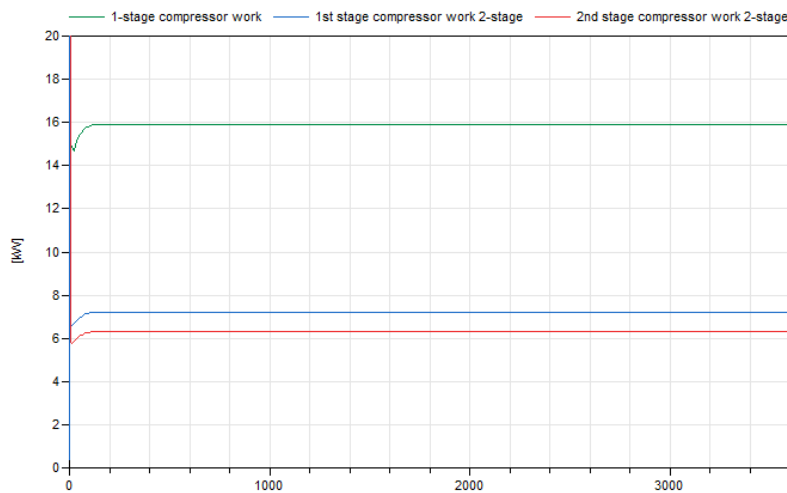


Figure 30: Compressor work in single-stage and two-stage mode

Figure 31 and 32 shows the log Ph diagrams for the two simulations. In these diagrams, the heat loss from the compressor, as well as the effect of the

desuperheater is clearer than what was the case for the 16th of May. For the single-stage cycle, the enthalpy difference between the two red marks at the top right of the cycle is the heat loss from the compressor. The heat loss from the compressors for this simulation can be calculated from equation 13:

$$\dot{Q}_{\text{loss}} = (h_2 - h_3) * \dot{m} = \left(1974 \frac{\text{kJ}}{\text{kg}} - 1820 \frac{\text{kJ}}{\text{kg}}\right) * 0.084 \frac{\text{m}}{\text{s}} = 12.94 \text{kW} \quad (13)$$

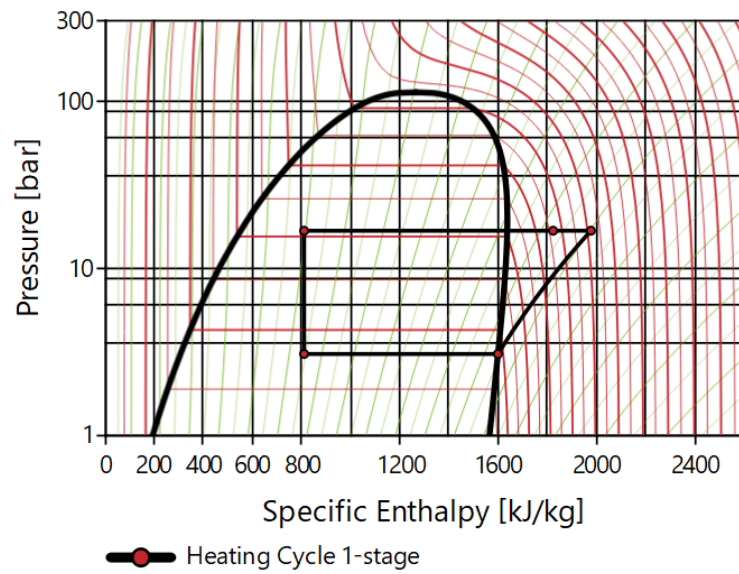


Figure 31: Log Ph diagram of the single-stage cycle

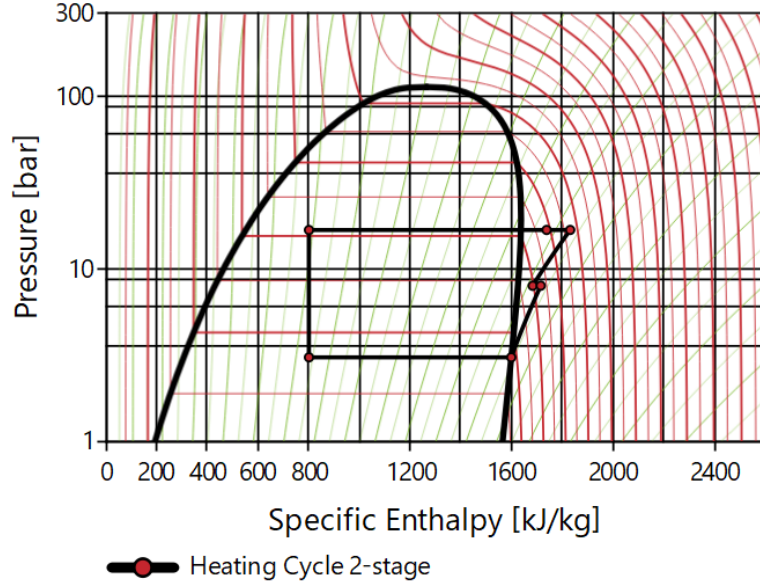


Figure 32: Log Ph diagram of the two-stage cycle

From the values found from the simulations, the COP can be calculated to find the performance of the system in heating mode. This is shown in equation 14 and 15.

$$COP_{\text{heating single-stg}} = \frac{\dot{Q}_{\text{cond}}}{\dot{W}_{\text{comp}}} = \frac{85.18kW}{31.82kW} = 2.68 \quad (14)$$

$$COP_{\text{heating two-stg}} = \frac{\dot{Q}_{\text{cond}}}{\dot{W}_{\text{comp}}} = \frac{(80.01 + 2.76)kW}{27.08kW} = 3.06 \quad (15)$$

The simulation of two-stage operation has a 14.2% higher COP than for the single-stage simulation. This is a larger difference than for the 16th of May, which was 9.6%. This is to be expected, as the pressure ratio for the 28th of January is 5.47, while it is 2.65 for the 16th of May.

6.2.2 Cooling Mode

The mass flow for the single-stage compression simulation was found to be 0.084 kg/s. For the two-stage compression simulation, the mass flow was also found to be 0.084 kg/s. Both these values are equal to the results from the real heat pump.

From the simulations, the cooling delivered from the evaporator have been found. These values are shown in figure 33. For the single-stage compression simulation, the delivered cooling is found to be 73.12 kW. This is slightly higher than the value found from ClimaCheck, which was 72.22 kW.

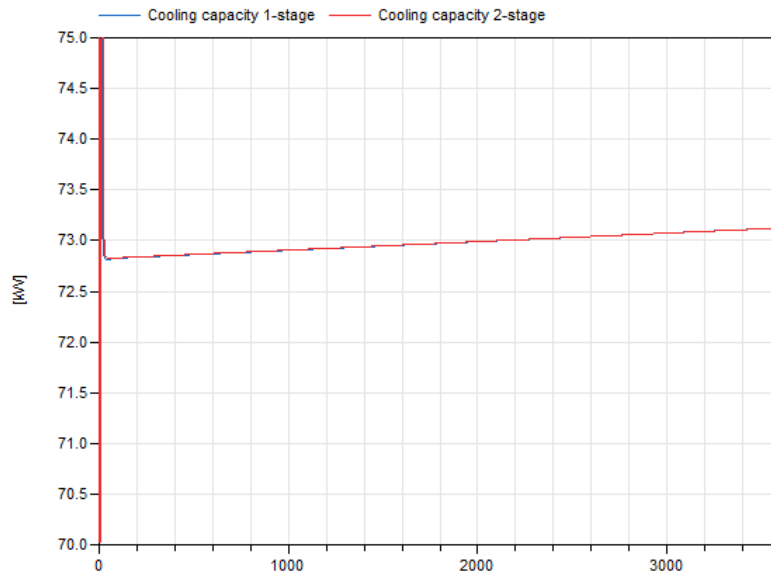


Figure 33: Cooling capacity of the heat pump with single-stage and two-stage compression

As can be seen from the figure, the cooling capacity delivered from the two-stage simulation is identical to that of the single-stage simulation. There is a slight increase in cooling delivered as the system runs. This increase is very slow, and will not effect the system with normal operation, as the heat pump does not run for this long with continuous operation.

The compression work found for the single-stage compression is 31.82 kW, which is the same as for the heating operation. This can be seen in figure 34.

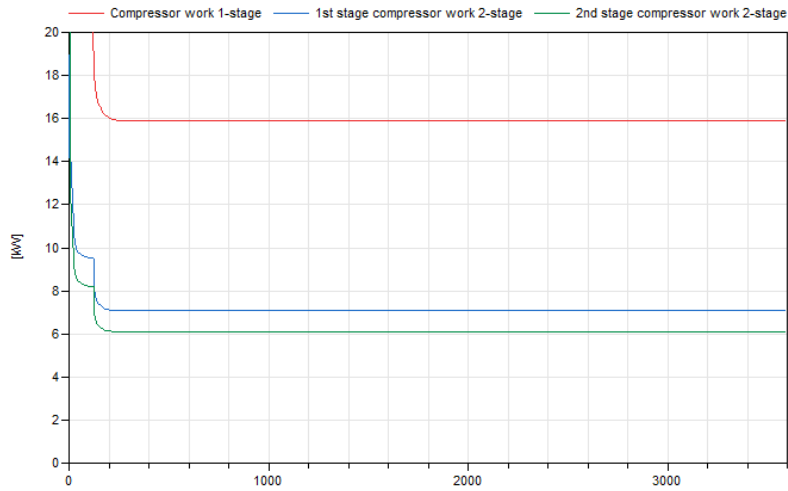


Figure 34: Compressor work in single-stage and two-stage mode

For the two-stage compression however, the results differ slightly from the heating mode operation. The results found from this simulation was 7.11 kW for the first stage, and 6.20 kW for the second stage. In total the compressor work for this simulation was 26.62 kW. This is lower than the work found in heating mode, which was 27.08 kW. The main reason for this is the slightly reduced refrigerant mass flow rate in this simulation, compared to that of the heating mode.

Following in figure 35 and 36, is the log Ph diagrams of the simulated heat pump operation for single-stage and two-stage compression. The main difference of these diagrams compared to the log Ph diagrams presented earlier in the report, is the sub-cooling. There is substantial sub-cooling in these simulations, found to be 43°C. This is because the condenser now is air-chilled, and the average outside air temperature for this time period was -5.71°C.

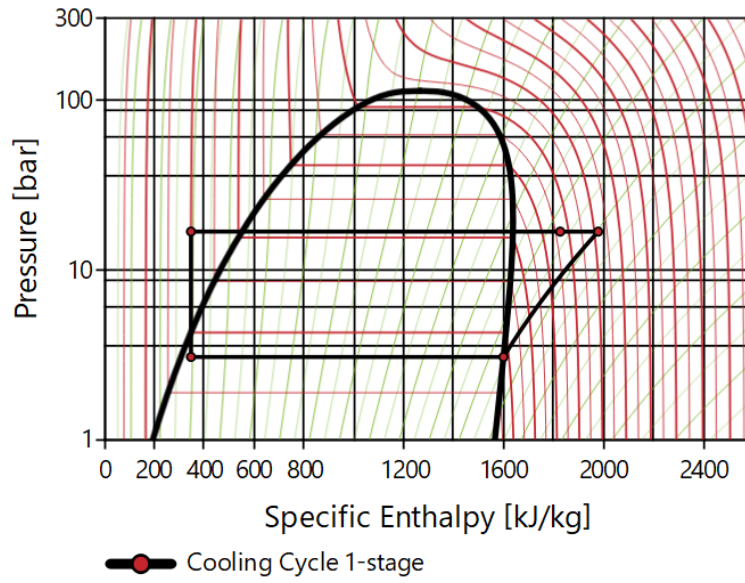


Figure 35: Log Ph diagram of the single-stage cycle

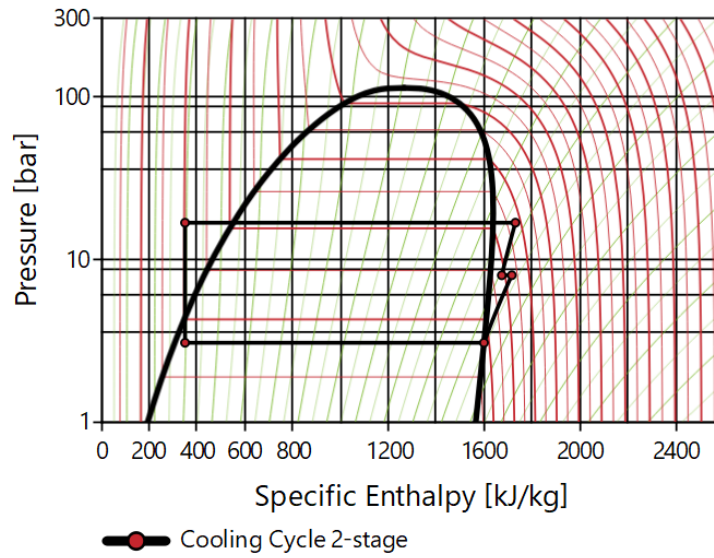


Figure 36: Log Ph diagram of the two-stage cycle

From the values found from the simulations, the COP can be calculated. This is shown in equation 16 and 17.

$$COP_{\text{cooling single-stg}} = \frac{\dot{Q}_{\text{evap}}}{\dot{W}_{\text{comp}}} = \frac{73.12kW}{31.82kW} = 2.30 \quad (16)$$

$$COP_{\text{cooling two-stg}} = \frac{\dot{Q}_{\text{evap}}}{\dot{W}_{\text{comp}}} = \frac{73.12kW}{26.62kW} = 2.75 \quad (17)$$

The two-stage compression simulation has a 19.6% higher COP value than that of the single-stage compression. This is a significant increase in performance by using two-stage compression instead of single-stage.

To better demonstrate the performance of the heat pump for the given time frame, the bar graph in figure 37 shows the average performance of the heat pump in the given time frame which is investigated in this chapter.

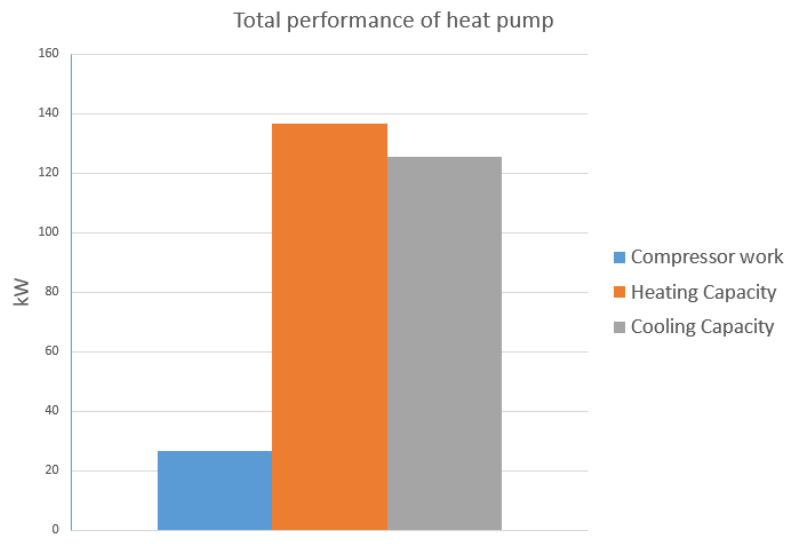


Figure 37: Average delivered heating and cooling compared to the compressor work

7 Discussion

The simulations have provided clear indications as to how two-stage compression would affect the performance of the system, compared to the single-stage operation that is the main setting of the system.

7.1 Single-stage versus two-stage compression

For both the 16th of May and the 28th of January, the results from the simulations provided clear results that favoured two-stage compression compared to single-stage compression, which was the setting used for both of these days.

The two-stage compression work was higher than the measured compressor work for the real system for all the simulations. There is, however, probably something wrong with the results from ClimaCheck. By calculating the compressor work from using the isentropic efficiency, pressure lift, and isentropic efficiency provided from the same result sheet, the calculated compressor work was almost identical to the simulated results for single-stage compression for all the different settings.

The desuperheater worked as intended for these simulations, although the heat removed from the gas was not substantial. The two days inspected through this report were of the warmest and coldest days of the year. For operation on days with more normal temperature levels, the pressure lift will not be as high as in these cases. For these days, the desuperheater might actually reduce the performance of the system. In the simulations for the 16th of May, the temperature difference between the inlet temperature of the refrigerant and the water into the desuperheater was only 0.46°C . For days with a lower pressure ratio than that of this day, the desuperheater will actually heat up the gas additionally before the second compressor stage.

7.2 Compressor heat loss

The heat loss from the compressor found from simulations and comparison with the results from the actual heat pump were significant. For the 28th of January, the heat loss was calculated to be 12.94 kW for the single-stage

compression simulation. This is almost a third of the compressor work of 31.82 kW. A solution that could be implemented to reduce the heat loss from the compressor is to add an insulation layer around parts of the compressor. The potential reduction in heat loss from this improvement is not covered in this report, and would have to be investigated further if this was to be considered.

7.3 Secondary fluid flow rate

Some values found for the mass flow of the secondary fluid through the condenser and evaporator were extremely high. For the time frame examined for the 16th of May, the average mass flow of water through the condenser was 27.62 kg/s, while through the evaporator it was 19.03 kg/s. It is possible that there is something wrong with the sensors measuring these values, but it has to be addressed. If these results are accurate, the work spent by the pumps would be significant.

The ΔT for the water stream from the evaporator inlet to outlet for the cooling simulation for the 28th of January is found to be 0.03°C. This value is for a cooling capacity of 72.2 kW. By lowering the water mass flow through the evaporator, the ΔT would increase. Because of the low value of the ΔT in this instance, the water mass flow could be reduced significantly without notably impacting the cooling delivery of the evaporator.

7.4 Economic evaluation

From the 16th of May 2018 to the 16th of May 2019, the total energy spent by the compressors was found through ClimaCheck to be 17 434 kWh. This value seemed to be abnormally small, and by investigating the compressor work through the year, it was found that, according to ClimaCheck, the compressors were turned off up until the 25th of December. This is shown in figure 38. Except for one day in September, one in June and one in May, this was the case from the 17th of April 2018. This is obviously a fault in the results, since the other values found for this time period showed that the heat pump was in use. By using the average compressor work during the time period where the compressor was on from the 7th of January until the 16th of May, the yearly energy spent by the compressors was estimated to be 84 393 kWh.

This is only an approximation, but can be used in the following calculations to give an indication to the possible energy savings and economical benefits of using two-stage compression more than is the case at this time.

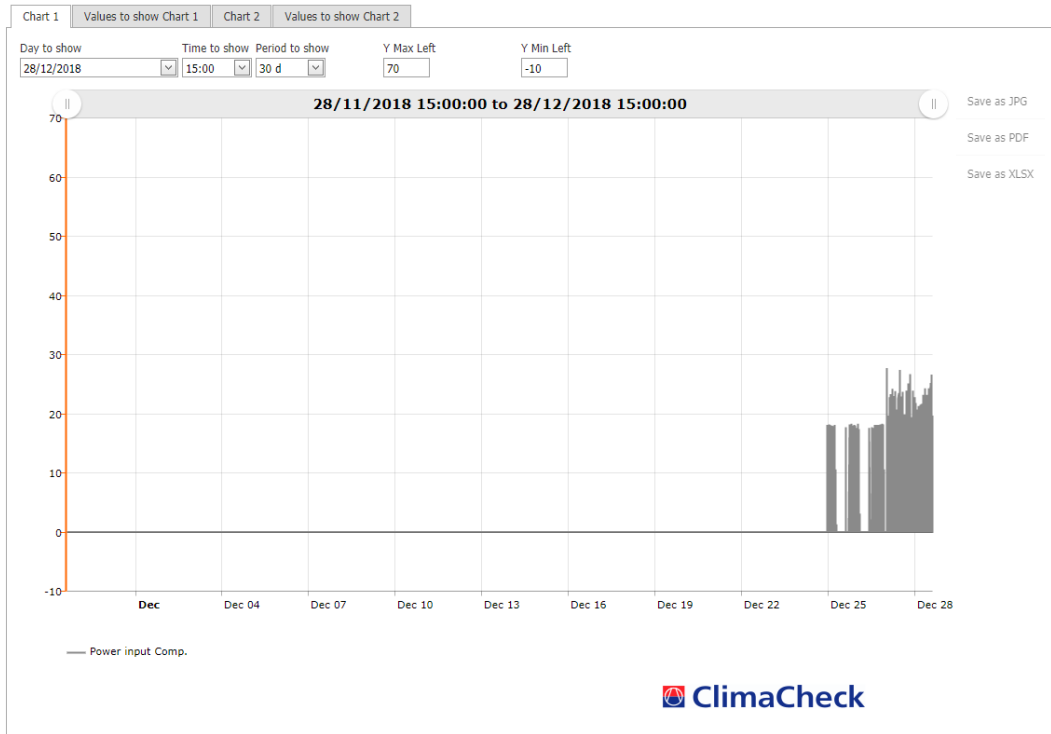


Figure 38: Compressor work for a month from ClimaCheck

The number of days where two-stage compression would be a viable alternative to single-stage compression is not clear through the results found in this report. To find the number of days where two-stage compression would be preferable, more simulations would be needed to find the exact outside temperatures where it should be used. This would also have to be compared to weather statistics for Bergen to find the number of days with temperatures where two-stage compression should be used. To examine if this work should be done, a simplified economic evaluation has been made. For this evaluation the hottest 5% and the coldest 5% of the days has been assumed to be the number of days where two-stage compression should be used.

The energy saving found from the results varied from 9.5% to 19.6%. Since these are the hottest and coldest days found, the average energy saved would be lower. For this calculation, an average energy reduction of 10% has been assumed to give an indication to potential economical benefits of switching

to two-stage compression. The total average cost for 1 kWh of electricity is, according to SSB, 0.856 Norwegian Kroner (Statistisk Sentralbyrå, 2019).

From this, an approximate calculation of yearly savings can be performed. The energy spent by the compressors in the 10% where it is assumed that the heat pump could perform better with two-stage compression, is 8439.3 kWh. From this, with an average energy reduction of 10%, the energy saved by switching to two-stage compression would be 843.9 kWh.

$$\text{Yearly Savings} = 843.9 \text{ kWh} * 0.856 \frac{\text{NOK}}{\text{kWh}} = 722.4 \text{ NOK} \quad (18)$$

This is a very simplified economic evaluation, but is included to show that the possible economic advantages to changing the settings of the heat pump are vanishingly small. From these findings, it would not be beneficial for GK to spend any resources on changing the settings of the heat pump. The hours spent to change these settings would more than likely give a potential payback period of several years. This also shows that there is not a high enough potential economical benefit to warrant spending a lot of time researching the exact number of days where two-stage compression should be used to find the exact value of the yearly savings.

8 Conclusion

The simulation results from the simplified model shows that the single-stage model provides a good basis to compare with the two-stage compression simulations. The results from the simulations of the single-stage system are almost identical to the results found from ClimaCheck. There are, however, evident flaws with the measurements and results from the ClimaCheck system. The results for the work of the compressor do not coincide with the theoretical work with the given pressure lift, isentropic efficiency and refrigerant mass flow. In several instances, it was found from the ClimaCheck results that the compressor isentropic efficiency was as high as 120 %. The conclusion derived from this is that the results from ClimaCheck do not give an accurate representation of the actual performance of the heat pump. The results found in the report do, however, provide a basis for further research into the ClimaCheck controls.

Another finding of the report, shed light on one factor that should be considered changing; namely the water mass flow through the condenser and evaporator. Results found from ClimaCheck indicate that the mass flow is often very high. This means that there is a lot of energy being spent in the pumps. By having a lower mass flow, and a larger ΔT from the water inlet to outlet, the pump work could be reduced, and thereby the efficiency of the system would increase.

By comparing the simulation results for single-stage and two-stage compression, it was found that the performance was higher for the two-stage compression in each of the simulations. The increase in COP when switching to two-stage compression varied from 9.5% to 19.6%. This shows that changing the settings of the heat pump to two-stage compression, offers energy saving potential not only when the temperature is below -10, but also in milder temperature conditions that are more common in Bergen throughout the year.

The potential economical benefit by changing these settings however, is too small to justify spending time or resources in order to make changes to the heat pump. To get clear results of the actual environmental and economical benefits of changing the settings of the heat pump, the heat pump has to be tested with both single-stage and two-stage compression at different ambient conditions. There were no results from ClimaCheck with two-stage compression, so to

make sure of the effect of switching to two-stage compression, the heat pump would have to be tested in this operation. The results from this report however, indicate that the benefits of conducting such tests are small, if not negligible. As such, while performing such tests could be interesting from an academic point of view, they are not likely to yield benefit economically.

9 Recommendations for Future Work

The models created for this report does give insight into the performance of the heat pump. There is however room for improvement of the models. If possible, a model of the system with simultaneous heating and cooling should be made. This would provide even more accurate results, as it would better represent the actual system.

The results found through simulations in this report gives an indication of the performance of the heat pump and possible improvements to the system. To find the actual performance and potential energy savings from making changes to the settings of the heat pump, systematic testing of the heat pump have to be conducted. The potential energy savings by lowering the mass flow of the secondary fluid through the heat exchangers should also be investigated to evaluate the potential benefits of changing this mass flow.

An examination of the results given by the ClimaCheck website, found that these were often inaccurate. Whether this has something to do with the calculations, or flaws associated with the sensors in the system, is not clear. This should be investigated further, and proper adjustments should be made to get correct results. This could also make the heat pump more efficient, as ClimaCheck controls the settings of the heat pump.

Switching to two-stage compression for particularly cold and hot days will save energy according to the simulations in this report. However, this is simulated results, and will differ some from the actual heat pump. To accurately examine how much energy can be saved by changing the settings for when the compressor has two-stage compression, the real heat pump has to be tested with both single-stage and two-stage compression at different conditions. The results found in this report does, however, indicate that doing these tests would be of a more academical interest than an economical one.

References

- P. Muthukumar B. Kiran Naik. Empirical correlation based models for estimation of air cooled and water cooled condenser's performance. 2016.
- Opeyemi Bamigbetan et al. Review of vapour compression heat pumps for high temperature heating using natural working fluids. 2017.
- James N. Pitts Jr Barbara J. Finlayson-Pitts. *Chemistry of the Upper and Lower Atmosphere*, pages 657–726. 2000.
- Kaja Wright Bergwitz-Larsen. Energy efficient and environmental friendly snow production by refrigeration systems. master thesis, NTNU. 2017.
- P C. Koelet and T B. Gray. *Compressors*, pages 73–131. 1992. ISBN 978-1-349-11435-1. doi: 10.1007/978-1-349-11433-7_4.
- Trygve M Eikevik. Compendium tep4255, chapter 1, introduction. 2015a.
- Trygve M Eikevik. Compendium tep4255, chapter 3, thermodynamic analysis. 2015b.
- Trygve M Eikevik. Compendium tep4255, chapter 4, working fluids. 2015c.
- V Gudjonsdottir et al. Enhanced performance of wet compression-resorption heat pumps by using nh₃-co₂-h₂o as working fluid. 2017.
- K Hoffmann and D.F. Pearson. Ammonia heat pumps for district heating in norway—a case study. 2011.
- Jonas K Jensen et al. Technical and economic working domains of industrial heat pumps: Part 2 – ammonia-water hybrid absorption-compression heat pumps. 2015.
- Jonas K Jensen et al. Design of serially connected district heating heat pumps utilising a geothermal heat source. 2017.
- Srinivas Garimella John G. Bustamante, Alexander S.Rattner. *Applied Thermal Engineering*, pages 362–371. 2016.
- Minsung Kim et al. Design of a high temperature production heat pump system using geothermal water at moderate temperature. 2010.
- Sunjae Kime et al. Performance optimization of an r410a air-conditioner with

- a dual evaporator ejector cycle based on cooling seasonal performance factor. 2018.
- Mattias Krysanter et al. Diagnosis analysis of modelica models. 2018.
- Dietmar Winkler Martin Otter. Modelica overview. 2013.
- Mark O McLinden et al. A thermodynamic analysis of refrigerants: Possibilities and tradeoffs for low-gwp refrigerants. 2014.
- Gert Nielsen. Vba code. gert.nielsen@xrgy.no.
- NOVAP. Energibruken i bygg kan effektiviseres mer enn 40 prosent. <https://www.novap.no/artikler/energibruken-i-bygg-kan-effektiviseres-mer-enn-40-prosent>. Accessed: 21.05.2019.
- Bjørn Palm. Ammonia in low capacity refrigeration and heat pump systems. 2008.
- J.M. Rodriguez. *Treatise on Geochemistry Vol 4*, chapter 4.14. 2007.
- Eskil Selvåg. Analyse av varmpumpeanlegg i nærvarmesystem. master thesis, NTNU. 2007.
- Statistisk Sentralbyrå. Elekrisitetspriser. <https://www.ssb.no/elkraftpris/>, 2019. Accessed: 25.05.2019.
- Jørn Stene. IEA annex 22 compression systems with natural working fluids, final report. 1998.
- Jørn Stene. Design and application of ammonia heat pump systems for heating and cooling of non-residential buildings. 2008.
- United Nations. About montreal protocol. <https://www.unenvironment.org/ozonaction/who-we-are/about-montreal-protocol>, 2016. Accessed: 20.05.2019.
- United Nations. Global environmental outlook. 2019.
- Wei Wu et al. A potential solution for thermal imbalance of ground source heat pump systems in cold regions: Ground source absorption heat pump. 2013.

Wei Wu et al. Hybrid ground source absorption heat pump in cold regions: Thermal balance keeping and borehole number reduction. 2015.

Wei Wu et al. Experimental investigation on nh₃-h₂o compression-assisted absorption heat pump (cahp) for low temperature heating under lower driving sources. 2016.

Wei Wu et al. Progress in ground-source heat pumps using natural refrigerants. 2018.

Alexandrs Zajacs et al. Small ammonia heat pumps for space and hot tap water heating. 2017.

Appendix

A Components in Modelica

A.1 Air heat exchanger in model

General Add modifiers Attributes

Component

Name

Comment

Model

Path TIL.HeatExchangers.FinAndTube.Geometry.FinAndTubeGeometry

Comment Geometry of fin and tube heat exchanger

Icon


Fin Side Geometry

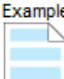
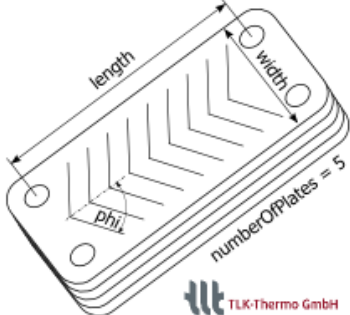
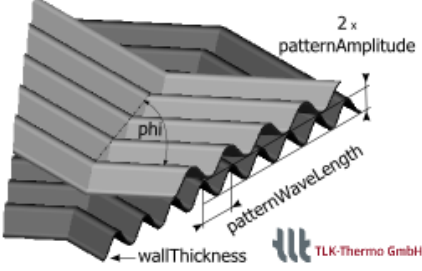
finnedTubeLength	<input type="text" value="0.515"/>	m	Length of finned tubes
nSerialTubes	<input type="text" value="21"/>		Number of serial tubes
serialTubeDistance	<input type="text" value="0.01"/>	m	Distance between serial tubes
nParallelTubes	<input type="text" value="20"/>		Number of parallel tubes
parallelTubeDistance	<input type="text" value="0.5"/>	m	Distance between parallel tubes
finThickness	<input type="text" value="0.02"/>	m	Thickness of fins
finPitch	<input type="text" value="0.02"/>	m	Distance between fins

Tube Side Geometry

tubeInnerDiameter	<input type="text" value="0.01"/>	m	Inner diameter of tube
tubeWallThickness	<input type="text" value="0.001"/>	m	Thickness of tube walls
nTubeSideParallelHydraulicFlows	<input type="text" value="1"/>		Number of parallel tube side flows

A.2 Condenser in heating mode

General	SIM	Advanced	Initialization	Advanced Initialization	Start Values	Add modifiers	Attributes
Component							
Name	parallelFlowHX						
Comment							
Model							
Path	TIL.HeatExchangers.Plate.VLEFluidLiquid.ParallelFlowHX						
Comment	Plate vle fluid liquid parallel flow HX						
Icon							
							
General							
hxGeometry	redeclare TIL.HeatExchangers.Plate.Geometry.Example hxGeometry(length=0.719, width=0.470, i					Geometry	
nCells	3					Number of cells in each path	
VLE Fluid							
HeatTransferModel_a	TIL.HeatExchangers.Plate.TransportPhenomena.HeatTransfer.ConstantAlpha (constantAlpha=2500)					Heat transfer model	
PressureDropModel_a	TIL.HeatExchangers.Plate.TransportPhenomena.PressureDrop.ZeroPressureDrop					Pressure drop model	
Liquid							
HeatTransferModel_b	TIL.HeatExchangers.Plate.TransportPhenomena.HeatTransfer.ConstantAlpha (constantAlpha=1500)					Heat transfer model	
PressureDropModel_b	TIL.HeatExchangers.Plate.TransportPhenomena.PressureDrop.ZeroPressureDrop					Pressure drop model	
Wall							
WallMaterial	TILMedia.SolidTypes.TILMedia_Steel					Wall material	
WallHeatConductionModel	TIL.HeatExchangers.Plate.TransportPhenomena.WallHeatTransfer.GeometryBasedConduction					Heat transfer model	

General		Add modifiers	Attributes
Component			
Name	<input type="text" value="redeclare hxGeometry"/>		Icon 
Comment	<input type="text"/>		
Model			
Path	TIL.HeatExchangers.Plate.Geometry.Example		
Comment	Example plate heat exchanger geometry		
Geometry outside			
numberOfPlates	<input type="text" value="95"/>	▶	Total number of plates
length	<input type="text" value="0.719"/>	▶ m	Plate length
width	<input type="text" value="0.470"/>	▶ m	Plate width
phi	<input type="text" value="35"/>	▶	Pattern angle in deg
			
Geometry inside			
wallThickness	<input type="text" value="0.75e-3"/>	▶ m	Wall thickness
patternAmplitude	<input type="text" value="2e-3"/>	▶ m	Pattern amplitude
patternWaveLength	<input type="text" value="12.6e-3"/>	▶ m	Pattern wave length
			

A.3 Evaporator in cooling mode

General SIM Advanced Initialization Advanced Initialization Start Values Add modifiers Attributes

Component


Name

Comment

Model

Path TIL.HeatExchangers.Plate.VLEFluidLiquid.ParallelFlowHX

Comment Plate vle fluid liquid parallel flow HX

Icon 

General

hxGeometry Geometry

nCells Number of cells in each path

VLE Fluid

HeatTransferModel_a Heat transfer model

PressureDropModel_a Pressure drop model

Liquid

HeatTransferModel_b Heat transfer model

PressureDropModel_b Pressure drop model

Wall

WallMaterial Wall material

WallHeatConductionModel Heat transfer model

OK Cancel Info

General Add modifiers Attributes

Component

Name

Comment

Model

Path TIL.HeatExchangers.Plate.Geometry.Example

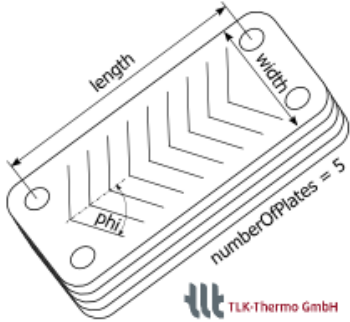
Comment Example plate heat exchanger geometry

Icon

Example

Geometry outside

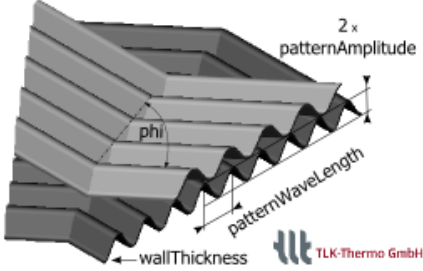
numberOfPlates	<input type="text" value="41"/>	▶	Total number of plates
length	<input type="text" value="0.719"/>	▶ m	Plate length
width	<input type="text" value="0.470"/>	▶ m	Plate width
phi	<input type="text" value="35"/>	▶	Pattern angle in deg



TLK-Thermo GmbH


Geometry inside

wallThickness	<input type="text" value="0.75e-3"/>	▶ m	Wall thickness
patternAmplitude	<input type="text" value="2e-3"/>	▶ m	Pattern amplitude
patternWaveLength	<input type="text" value="12.6e-3"/>	▶ m	Pattern wave length




TLK-Thermo GmbH

A.4 Compressor

General	SIM	Advanced	Add modifiers	Attributes
Component				
Name	effCompressor2			
Comment				
Model				
Path	TIL.VLEFluidComponents.Compressors.EffCompressor			
Comment	Efficiency based compressor model			
Icon				
				
Mechanics				
use_mechanicalPort	<input type="checkbox"/> true	▾	= true, if mechanical port is used	
nFixed	<input type="text" value="20"/>	▾	Hz	Speed
displacement	<input type="text" value="1.2e-3"/>	▾	m3	Displacement
use_relDisplacementInput	<input type="checkbox"/> false	▾	= true, if relative displacement input connector is used	
Compressor Efficiencies				
volumetricEfficiency	<input type="text" value="0.88"/>	▾	1	Volumetric efficiency
isentropicEfficiency	<input type="text" value="0.798"/>	▾	1	Isentropic efficiency
effectiveIsentropicEfficiency	<input type="text" value="0.798"/>	▾	1	Effective isentropic efficiency

A.5 PI-controller

General		Advanced	Add modifiers	Attributes
Component				Icon
Name	<input type="text" value="piController4"/>			
Comment	<input type="text"/>			
Model				
Path	TIL.OtherComponents.Controllers.PIController			
Comment	PI-Controller with optional inputs for gain scheduling			
Settings				
controllerType	<input type="text" value="PI"/>	▶	Controller Type	
invertFeedback	<input type="text" value="false"/>	▶	true, if feedback signal is inverted	
offset	<input type="text" value="0.0"/>	▶	Operating point, added to proportional output	
integralParameterType	<input type="text" value="Ti"/>	▶	Controller Structure $[k*(u + 1/Ti*integral(u))]$ or $[k*u + ki*integral(u)]$	
Setting parameters				
k	<input type="text" value="1"/>	▶	Proportional gain of controller	
Ti	<input type="text" value="0.1"/>	▶ s	Time constant of Integrator block	
ki	<input type="text" value="0.5"/>	▶ s-1	Integral gain	
Limits				
yMax	<input type="text" value="300"/>	▶	Upper limit of output	
yMin	<input type="text" value="1"/>	▶	Lower limit of output	
Initialization				
initType	<input type="text" value="initialOutput"/>	▶	Type of initialization	
yInitial	<input type="text" value="50"/>	▶	Initial output of controller	
Activation				
use_activeInput	<input type="text" value="false"/>	▶	= true, if controller is switched on/off externally	
use_y_notActive	<input type="text" value="false"/>	▶	= true, if output of not activated controller is defined externally. Otherwise output is hold at deactivation.	
activationTime	<input type="text" value="0.0"/>	▶ s	Time when controller is switched on	

B Results from ClimaCheck

B.1 16th of May

()	Typ	Ref Low press. (Bar(g))		Ref High press. (Bar(g))		Ref Evap (°C)		Ref Comp in (°C)		Ref Cond (°C)		Ref Comp out (°C)		Eff 2 Comp. Isen. (%)		Power input Comp. (kW)		COP Cool		Cap. Cool (kW)		Heat (kW)	
		PT_RLP	PT_RHP	RLP_IEVA	IT_RCMP	IT_RCMP	RHP_ICOM	D_MID	IN	OUT	IT_RCMP	OUT	ISEN	COMP_EFF	EP_COMP	OL	REF	OL	RCOP_CO	RCAP_CO	OL	HEAT	RCAP_H
2019-05-16 12:54:25	5,28	13,44	10,64	11,6	37,38	78,6	61,79	23,45	5,84	137,05	6,57	154,13											
2019-05-16 12:53:28	5,05	13,85	9,58	11,6	38,36	78,6	68,88	23,34	5,98	139,5	6,7	156,43											
2019-05-16 12:52:25	5,04	14,04	9,58	11,7	38,83	78,9	70,64	23,67	6	141,93	6,72	159,15											
2019-05-16 12:51:25	5,31	13,76	10,82	11,7	38,15	78,9	63,23	23,81	5,84	139,16	6,57	156,49											
2019-05-16 12:50:25	5,12	13,96	9,92	11,7	38,62	78,9	68,31	23,32	5,95	138,69	6,68	155,66											
2019-05-16 12:49:25	5,03	14,37	9,48	11,7	39,61	78,9	74	24,33	6,1	148,32	6,75	164,14											
2019-05-16 12:48:25	5,07	13,91	9,66	11,7	38,51	79,1	68,59	23,45	5,94	139,35	6,67	156,37											
2019-05-16 12:47:25	5,04	14	9,51	11,7	38,72	79,5	69,17	23,6	5,91	139,4	6,63	156,5											
2019-05-16 12:32:25	5,29	16,1	10,72	12,2	43,48	84,8	72,07	25,34	5,44	137,8	6,16	155,97											
2019-05-16 12:31:25	5,13	16,16	9,98	12,2	43,62	84,8	75,11	23,96	5,47	131,09	6,12	146,67											
2019-05-16 12:30:25	5,45	15,85	11,43	12,2	42,93	84,4	67,25	24,1	5,31	127,9	6,01	144,96											
2019-05-16 12:29:25	5,44	15,64	11,41	12,2	42,48	84	65,52	21,21	5,25	111,45	5,95	126,25											
2019-05-16 12:28:25	5,17	16,07	10,15	12,1	43,42	83,9	72,59	21,96	5,37	117,88	6,06	133,05											
2019-05-16 12:27:25	5,15	16,16	10,06	12,1	43,62	83,9	74,53	21,91	5,46	119,65	6,14	134,45											
2019-05-16 12:26:25	5,16	16,14	10,12	12,1	43,58	83,8	74,64	21,61	5,49	118,6	6,15	132,95											
2019-05-16 12:25:25	5,15	16,19	10,06	12	43,67	83,8	74,06	21,77	5,41	117,79	6,11	132,91											
2019-05-16 12:24:25	5,48	15,46	11,57	12	42,08	83,8	64,57	21,89	5,29	115,84	6	131,32											
2019-05-16 12:22:25	5,21	16,06	10,32	11,9	43,4	83,4	72,98	21,34	5,44	116,03	6,14	130,94											
2019-05-16 12:21:28	5,26	16,01	10,58	11,9	43,29	83,2	71,67	21,07	5,41	114,07	6,11	128,74											
2019-05-16 12:20:25	5,14	16,13	10,01	11,9	43,54	82,9	76,56	22,07	5,49	121,14	6,14	135,49											
2019-05-16 12:18:25	5,14	15,98	10,03	11,8	43,23	82,5	75,35	21,72	5,54	120,43	6,19	134,55											
2019-05-16 12:17:25	5,33	15,61	10,89	11,8	42,42	82,3	69,84	21,42	5,49	117,69	6,2	132,82											
2019-05-16 12:16:25	5,08	16,34	9,71	11,7	44	81,5	80,15	21,92	5,36	117,54	6,01	131,78											
2019-05-16 12:15:25	5,44	15,62	11,4	11,8	42,43	80,1	70,87	21,31	5,7	121,45	6,4	136,49											
2019-05-16 12:14:25	5,15	15,94	10,04	11,9	43,13	83,11	83,11	21,54	5,56	119,82	6,21	133,82											
2019-05-16 12:13:25	5,14	15,81	10,02	11,9	42,86	76,4	87,02	21,44	5,6	120,17	6,25	134,1											
2019-05-16 12:12:25	5,23	14,52	10,43	11,9	39,95	75,3	74,94	19,75	6,25	123,35	6,9	136,19											
2019-05-16 12:11:25	5,13	14,09	9,95	11,9	38,94	75,2	73,36	19,18	6,35	121,75	7	134,21											
2019-05-16 12:10:25	5,14	13,94	10,03	11,9	38,58	75,3	70,25	18,96	6,17	116,99	6,87	130,18											
2019-05-16 12:09:25	5,16	14,08	10,12	12	38,92	75,3	72,54	19,14	6,32	120,96	7,03	134,5											
2019-05-16 12:08:25	5,42	13,86	11,31	11,9	38,38	75,4	64,02	19,22	6	115,26	6,69	128,62											
2019-05-16 12:07:25	5,21	14,1	10,32	12	38,98	75,3	71,63	18,89	6,28	118,68	6,99	132,01											
2019-05-16 12:06:32	5,11	14,17	9,89	12	39,12	75,2	73,56	19,1	6,29	120,21	6,94	132,63											
2019-05-16 12:05:25	5,22	14,07	10,41	12	38,89	75,1	70,85	18,71	6,26	117,21	6,97	130,34											
	5,232222222	15,53444444	10,440556	11,980556	42,215	81,59166667	72,5997222	22,27888889	5,6144444	124,4767	6,3031	139,8133											

SMPTIME	RFLOW	SECC_FLOW_SECW_FLOW	TT_OUTDOOR	TT_RCOMP_OUT	TT_SECC_IN	TT_SECC_OUT	TT_SECW_IN	TT_SECW_OUT	
19-05-16 12:05:25	0,13	17,48	23,96	22,8	75,1	13,8	12,2	38,4	39,7
19-05-16 12:06:32	0,13	16,88	39,61	22,8	75,2	13,7	12	38,9	39,7
19-05-16 12:07:25	0,13	14,91	28,68	23,2	75,3	13,8	11,9	38,6	39,7
19-05-16 12:08:25	0,13	15,28	38,42	23,5	75,4	13,9	12,1	38,6	39,4
19-05-16 12:09:25	0,13	22,21	32,14	23,3	75,3	13,9	12,6	38,6	39,6
19-05-16 12:10:25	0,13	23,27	38,88	23	75,3	13,8	12,6	38,4	39,2
19-05-16 12:11:25	0,13	18,16	40,09	23	75,2	13,9	12,3	38,9	39,7
19-05-16 12:12:25	0,14	22,65	27,12	23,1	75,3	13,9	12,6	38,8	40
19-05-16 12:20:25	0,14	20,65	12,95	23,7	82,9	13,8	12,4	41	43,5
19-05-16 12:21:28	0,13	20,94	14,65	24	83,2	13,9	12,6	41,4	43,5
19-05-16 12:23:25	0,13	23,31	21,07	23,5	83,6	13,8	12,6	41,9	43,4
19-05-16 12:24:25	0,13	17,28	14,94	23,2	83,8	13,9	12,3	41,6	43,7
19-05-16 12:25:25	0,14	15,62	28,87	23,6	83,8	13,9	12,1	42,4	43,5
19-05-16 12:26:25	0,13	20,22	17,65	23,5	83,8	13,9	12,5	41,6	43,4
19-05-16 12:27:25	0,14	16,8	22,95	23,6	83,9	13,8	12,1	42,1	43,5
19-05-16 12:28:25	0,14	21,64	31,79	23,2	83,9	13,9	12,6	42,2	43,2
19-05-16 12:29:25	0,13	16,62	18,85	23,4	84	14	12,4	42	43,6
19-05-16 12:31:25	0,15	16,47	29,21	23,7	84,8	14,1	12,2	42,4	43,6
19-05-16 12:33:25	0,15	21,59	33,43	24,2	84,6	14,1	12,6	42,2	43,3
19-05-16 12:34:25	0,15	19,76	44,93	24,5	84,6	14,2	12,6	42,4	43,2
19-05-16 12:35:25	0,15	20,72	74,22	24,5	84,5	14,3	12,7	42,6	43,1
19-05-16 12:36:25	0,16	18,89	35,18	24,4	85	14,2	12,4	42,2	43,3
19-05-16 12:37:25	0,16	24,69	43,54	24,2	85,3	14,2	12,8	42,4	43,3
19-05-16 12:38:32	0,16	21,63	56,13	24,6	85,6	14,1	12,5	42,6	43,3
19-05-16 12:39:25	0,16	16,34	55,14	24,6	85,7	14,1	12	42,5	43,2
19-05-16 12:40:25	0,16	21,25	42,89	24,5	85,8	14	12,4	42,4	43,3
Average	0,1405556	19,028889	27,6197222	23,58888889	81,59166667	13,9416667	12,34166667	40,8777778	42,54722222

B.2 28th of January

() TYP	Ref Low press. (Bar(g))		Ref High press. (Bar(g))		Ref Evap (°C)		Ref Comp in Ref Cond (°C)		Ref Comp out (°C)		Eff 2 Comp. Ise. (%)		Power input Comp. (kW)		COP Ref		Cap. Cool (kW)		Cap. Heat (kW)	
	PT_RLP	PT_RHP	RLP	TI_RHP	TI_RCOMP	TI_RCOMP	TI_RCOMP	TI_RCOMP	TI_RCOMP	TI_RCOMP	ISEN	ISEN	EP_COMP	EP_COMP	OL	COOL	COOL	RCAP_COOL	RCAP_COOL	RCAP_HEAT
2019-01-28 05:49:42	2,01	15,99	-9,08	-6	43,25	113,2	65,82	25,44	3,27	83,23	3,87	98,35								
2019-01-28 05:48:42	1,98	15,96	-9,27	-6	43,18	112,7	68,22	27,19	3,27	88,91	3,92	106,58								
2019-01-28 05:47:42	1,99	15,94	-9,2	-5,9	43,14	112,1	68,42	27,08	3,28	88,77	3,93	106,37								
2019-01-28 05:46:42	2,01	15,7	-9,07	-5,9	42,6	111,5	66,14	25,27	3,32	83,95	3,92	99,09								
2019-01-28 05:45:46	2,01	15,86	-9,08	-5,8	42,95	111,4	66,97	25,11	3,3	82,84	3,94	98,94								
2019-01-28 05:44:42	1,99	15,86	-9,18	-5,8	42,97	111,1	67,14	25,02	3,29	82,31	3,93	98,44								
2019-01-28 05:43:42	1,99	15,84	-9,21	-5,7	42,91	110,7	67,96	25,2	3,29	82,95	3,94	99,33								
2019-01-28 05:42:42	1,98	15,81	-9,29	-5,6	42,84	110,2	68,98	25,15	3,29	82,74	3,94	99,08								
2019-01-28 05:41:42	1,98	15,83	-9,28	-5,5	42,89	109,5	69,83	25,45	3,29	83,66	3,94	100,21								
2019-01-28 05:37:42	2,03	15,77	-8,89	-5,1	42,76	106,3	69,75	22,55	3,33	75	3,98	89,66								
2019-01-28 05:36:42	2,06	15,74	-8,6	-5	42,71	105,7	69,52	22,33	3,35	74,83	4	89,34								
2019-01-28 05:35:42	2,11	15,97	-8,23	-5	43,19	105,5	69,58	21,93	3,35	73,44	4	87,7								
2019-01-28 05:34:42	2,18	15,88	-7,68	-4,9	43,01	104,7	70,77	23,5	3,4	80,01	4,05	95,28								
2019-01-28 05:16:42	2,04	16,04	-8,79	-5,7	43,35	109,3	67,73	23,56	3,3	77,65	3,95	92,96								
2019-01-28 05:15:42	2,04	15,89	-8,79	-5,7	43,02	108,7	68,55	24,66	3,32	81,78	3,97	97,81								
2019-01-28 05:14:42	2,04	15,82	-8,77	-5,6	42,87	107,9	68,65	24,6	3,33	81,88	3,98	97,87								
2019-01-28 05:13:45	2,04	15,79	-8,77	-5,6	42,8	106,8	69,38	24,35	3,33	81,15	3,98	96,97								
2019-01-28 05:12:42	2,09	15,57	-8,37	-5,5	42,32	106,1	64,86	21,41	3,34	71,55	3,9	83,58								
2019-01-28 05:11:42	2,1	15,67	-8,29	-5,6	42,54	106,3	62,07	19,49	3,19	62,23	3,73	72,72								
2019-01-28 05:10:42	2,06	15,78	-8,63	-5,7	42,78	106,9	63,28	19,81	3,21	63,55	3,75	74,32								
2019-01-28 05:09:42	2,03	15,99	-8,86	-5,7	43,24	107,2	66,45	21,37	3,3	70,47	3,88	82,85								
2019-01-28 05:08:42	2,04	15,94	-8,77	-5,7	43,14	106,8	67,64	22,36	3,31	74,03	3,96	88,57								
2019-01-28 05:07:42	2,04	15,93	-8,82	-5,6	43,12	106,5	68,51	22,06	3,31	72,96	3,96	87,3								
2019-01-28 05:06:42	2,05	15,99	-8,72	-5,6	43,24	105,9	69,03	22,29	3,31	73,73	3,96	88,21								
2019-01-28 05:05:42	2,05	15,94	-8,7	-5,5	43,14	105,2	70,35	22,48	3,32	74,54	3,97	89,15								
2019-01-28 05:04:42	2,05	15,92	-8,68	-5,4	43,1	104	70,86	22,11	3,32	73,39	3,97	87,77								
2019-01-28 05:03:42	2,07	15,74	-8,53	-5,5	42,71	103,1	67,2	20,01	3,36	67,17	3,97	79,37								
2019-01-28 05:02:42	2,09	15,68	-8,43	-5,3	42,56	102,3	67,93	20,2	3,37	68,17	4,02	81,29								
2019-01-28 05:01:42	2,1	15,72	-8,33	-5,3	42,65	101,9	66,31	19,05	3,38	64,32	3,93	74,89								
2019-01-28 05:00:42	2,09	15,69	-8,35	-5,3	42,59	101,7	66,6	18,97	3,38	64,09	3,95	74,9								
2019-01-28 04:59:42	2,09	15,71	-8,39	-5,3	42,64	101,4	67,85	19,19	3,37	64,7	4,01	76,94								
2019-01-28 04:58:49	2,1	15,81	-8,31	-5,4	42,85	100,9	68,19	19,12	3,37	64,34	4,02	76,77								
2019-01-28 04:57:42	2,12	15,79	-8,12	-5,3	42,82	100,7	68,66	19,13	3,38	64,69	4,03	77,13								
Average	2,0704	15,8306	-8,547	-5,518	42,8978	106,644	66,676	21,8334	3,3094	72,2242	3,9126	85,4712								

SMPTIME	RFLOW	SECC_FLOW_SECW_FLOW	TT_OUTDOOR	TT_RCOMP_OUT	TT_SECC_IN	TT_SECC_OUT	TT_SECW_IN	TT_SECW_OUT
19-01-28 04:56:42	0,07	5,22	-5,6	101,4	11,8	11,8	39,4	42,2
19-01-28 04:57:42	0,08	-154,4	-5,6	100,7	11,8	11,9	39,2	42,5
19-01-28 04:59:42	0,08	5,41	-5,8	101,4	11,9	11,9	38,9	42,3
19-01-28 05:01:42	0,08	5,77	-5,8	101,9	11,9	11,9	39,1	42,2
19-01-28 05:03:42	0,08	160,31	-5,8	103,1	12	11,9	38,8	42,3
19-01-28 05:05:42	0,09	5,61	-5,8	105,2	12	12	38,8	42,6
19-01-28 05:06:42	0,09	-175,95	-5,8	105,9	11,9	12	38,9	42,7
19-01-28 05:08:42	0,09	5,72	-5,8	106,8	12	12	38,9	42,6
19-01-28 05:27:42	0,08	5,54	-5,8	105,3	12,2	12,2	39,2	42,5
19-01-28 05:29:42	0,08	153,31	-5,7	105,1	12,3	12,2	39	42,5
19-01-28 05:31:42	0,08	31,75	-5,8	105	12,2	11,7	38,6	42,3
19-01-28 05:32:42	0,08	31,69	-5,7	104,9	12,1	11,6	38,4	42,2
19-01-28 05:33:42	0,08	32,12	-5,6	104,9	12,1	11,6	38,7	42,3
19-01-28 05:34:42	0,09	95,47	-5,6	104,7	12	11,8	38,5	42,2
19-01-28 05:36:42	0,09	-178,59	-5,8	105,7	11,7	11,8	38,4	42,2
19-01-28 05:37:42	0,09	5,1	-5,8	106,3	11,7	11,7	38,1	42,3
19-01-28 05:43:42	0,09	5,65	-5,8	110,7	11,9	11,9	38	42,2
19-01-28 05:46:42	0,09	4,83	-5,7	111,5	11,9	11,9	37,2	42,1
19-01-28 05:47:42	0,1	5,19	-5,6	112,1	11,9	11,9	37,6	42,5
19-01-28 05:48:42	0,1	5,42	-5,6	112,7	11,9	11,9	37,8	42,5
19-01-28 05:51:42	0,08	-164,82	-5,6	111,9	11,9	12	38,4	42,7
19-01-28 05:52:42	0,08	5,1	-5,7	110,8	12	12	38,7	42,6
19-01-28 05:53:42	0,08	5,28	-5,7	110	12	12	38,8	42,6
19-01-28 05:56:42	0,08	5,25	-5,9	108,4	12,1	12,1	38,9	42,3
19-01-28 05:57:42	0,08	5,17	-5,9	107,9	12,1	12,1	39	42,4
19-01-28 05:59:42	0,08	5,52	-5,8	106,9	12,1	12,1	38,4	42
	0,0844898	-54,296	-5,714285714	106,2795918	12,022449	11,98979592	38,644898	42,38571429

C Design values for the heat pump at Folke Bernadottes Vei 40

DRIFTSDATA FOR ANLÆGGET KØLE-DRIFT:

▪ <u>KØLEEFFEKT</u>	<u>420 kW</u>
▪ <u>OPTAGEN EFFEKT PÅ KOMPRESSOR</u>	<u>66 kW</u>
▪ <u>KAPACITETSREGULERING</u>	<u>FREKVENSOMFORMER + TRINUDKOBLING</u>
▪ <u>KOMPRESSOR COP</u>	<u>6,3 KØL</u>
▪	
▪ <u>FORDAMPNINGSTEMPERATUR</u>	<u>7,6 °C</u>
▪ <u>KØLEMIDDEL</u>	<u>NH₃</u>
▪ <u>MEDIE VÆSKESIDE</u>	<u>VAND</u>
▪ <u>TEMPERATURSÆT</u>	<u>17 °C / 10 °C</u>
▪ <u>FLOW</u>	<u>51.440 KG/H</u>
▪ <u>TRYKTAB VEKSLER</u>	<u>29 kPa</u>
▪	
▪ <u>KONDENSERINGSTEMPERATUR</u>	<u>39,4 °C</u>
▪ <u>LUFTTEMPERATUR</u>	<u>26 °C</u>
▪	
▪ <u>CA. DRIFTSVÆGT</u>	<u>13.000 KG</u>
▪ <u>STANDARD UDVENDIGE MÅL [L X B X H]</u>	<u>12.190 x 2.440 x 2.590 MM</u>
▪	
▪ <u>KOMPRESSOR COP VED 50 % LAST</u>	<u>CA. 9,2 KØL</u>
▪ <u>KOMPRESSOR COP VED 20 % LAST</u>	<u>CA. 11 KØL</u>
▪	
<u>MAX. KØLEYDELSE 1 KOMPRESSOR</u>	<u>CA. 300 kW</u>

DRIFTSDATA FOR ANLÆGGET VARMEPUMPE-DRIFT:

▪ <u>VARMEFFEKT</u>	<u>250 kW</u>
▪ <u>OPTAGEN EFFEKT PÅ KOMPRESSORER</u>	<u>30,9 + 37,0 kW</u>
▪ <u>KAPACITETSREGULERING</u>	<u>FREKVENSOMFORMER + TRINUDKOBLING</u>
▪ <u>KOMPRESSOR COP</u>	<u>3,68 VARME</u>
▪	
▪ <u>KONDENSERINGSTEMPERATUR</u>	<u>46 °C</u>
▪ <u>MEDIE VÆSKESIDE</u>	<u>VAND</u>
▪ <u>TEMPERATURSÆT</u>	<u>30 °C / 45 °C</u>
▪ <u>FLOW</u>	<u>14.360 KG/H</u>
▪ <u>TRYKTAB VEKSLER</u>	<u>27 kPa</u>
▪	
▪ <u>FORDAMPNINGSTEMPERATUR</u>	<u>-16 °C</u>
▪ <u>LUFTTEMPERATUR</u>	<u>-10 °C</u>
▪ <u>SOUND POWER LEVEL</u>	<u>91 dB(A)</u>
▪ <u>OPTAGEN EFFEKT EC VENTILATORER</u>	<u>12.000 W</u>
▪ <u>NOMINEL STRØMSTYRKE KONDENSATOR</u>	<u>18,6 A</u>
▪ <u>LAMELMATERIALE</u>	<u>SWR AL MG 2.5 (3,6 MM LAMELAFSTAND)</u>

D Heat pump function description

Folke Bernedottes vej 40

16-09-15

Indhold

Funktionsbeskrivelse:	1
Anlægget er udstyret med:.....	1
Kølefunktionen:	1
Varmefunktionen:	2
Mulighed for styring af afrimning med Trykvagt skal laves.....	3

Funktionsbeskrivelse:

Anlægget er konstrueret som køleanlæg/ Varmepumpe med kontinuerlig levering af kulde og varme, overskud/underskud af energi fra udeluften

Se venligst PI Diagram og ventilschema

Anlægget er udstyret med:

2 stk. (T)CMO 38 kompressorer som hver er Unisab 3 kontrolpanel og Frekvensomformer som varetager sikkerheds og kapacitets kontrol for anlægget

1 stk. M10 pladeveksler for kølevand 10/17°C

1 stk. M10 pladeveksler for varmt vand 30/45°C

Unisab 3 er tilsluttet BMS via Modbus

Kølefunktionen:

Når udetemperaturen T5 er over 14°C (justerbart) skiftes til:

1. signal til Unisab 3 (Control on "proces out") fra Modbus
Unisab 3 er kapacitets regulerende
Ventil V12-22-32-42 og V50 åbnes

Der gives 230v til "HB Control" væskedræn V11-21-31-41

2. Kondensator Fan reguleres efter PD1 10 bar (justerbart) til F10-20-30-40, 0-10V
3. Varmtvands temperatur reguleres efter T3 føler ved at stepvis åbne/ lukke V80 (overhednings fjerner)
Hvis temperaturen T3 ikke kan opnås, over længere tid 30 min.(Justerbart) reguleres Kondensatortrykket PD1 op stepvis, 2 bar, max. 16 bar.

Varmefunktionen:

Når udetemperaturen T5 er under 12°C (justerbart) skiftes til:

4. Signal til Unisab 3 (Control on "User 1") fra Modbus

Unisab 3 er kapacitets regulerende

Ventil V10-20-30-40 åbnes

Koldvands temperaturen reguleres efter T1 føler 10°C ved stepvis at åbne/ lukke V50

Fan hastighed sættes til 5v (Justerbart). når udetemperaturen T5 kommer under 2°C (justerbart) Sættes den til 10v

V80 lukkes

Afrimning: Opdeles i 3 segmenter.

Over 6°C (T5) ingen afrimning

Mellem 2 og 6°C (T5) luftafrimning 3X i døgnet eller manuelt

Energioptager 1 V10 Lukkes V11 åbnes og Fan fortsætter på 5v, efter 20 min (justerbart). Lukkes V11 og V10 Åbnes. Herefter følger,

Energioptager 2 V20 Lukkes V21 åbnes og Fan fortsætter på 5v, efter 20 min (justerbart). Lukkes 21 og V20 Åbnes. Herefter følger,

Energioptager 1 V30 Lukkes V31 åbnes og Fan fortsætter på 5v, efter 20 min (justerbart). Lukkes V31 og V40 Åbnes. Herefter følger,
Energioptager 1 V40 Lukkes V41 åbnes og Fan fortsætter på 5v, efter 20 min (justerbart). Lukkes V41 og V40 Åbnes.

Under 2^oc (T5)varmgas afrimning. 3X i døgnet eller manuelt

Energioptager 1: Fan F10 standses V10 lukkes, V11 og V12 åbnes Afsluttes efter tid (20 min justerbart) V11 og V12 lukkes V10 åbnes og F10 til max hastighed, herefter følger

Energioptager 2: Fan F20 standses V20 lukkes, V21 og V22 åbnes Afsluttes efter tid (20 min justerbart) V21 og V22 lukkes V20 åbnes og F20 til max hastighed, herefter følger

Energioptager 3: Fan F30 standses V30 lukkes, V31 og V32 åbnes Afsluttes efter tid (20 min justerbart) V31 og V32 lukkes V30 åbnes og F30 til max hastighed, herefter følger

Energioptager 4: Fan F40 standses V40 lukkes, V41 og V42 åbnes Afsluttes efter tid (20 min justerbart) V41 og V42 lukkes V40 åbnes og F40 til max hastighed.

Mulighed for styring af afrimning med Trykvagt skal laves

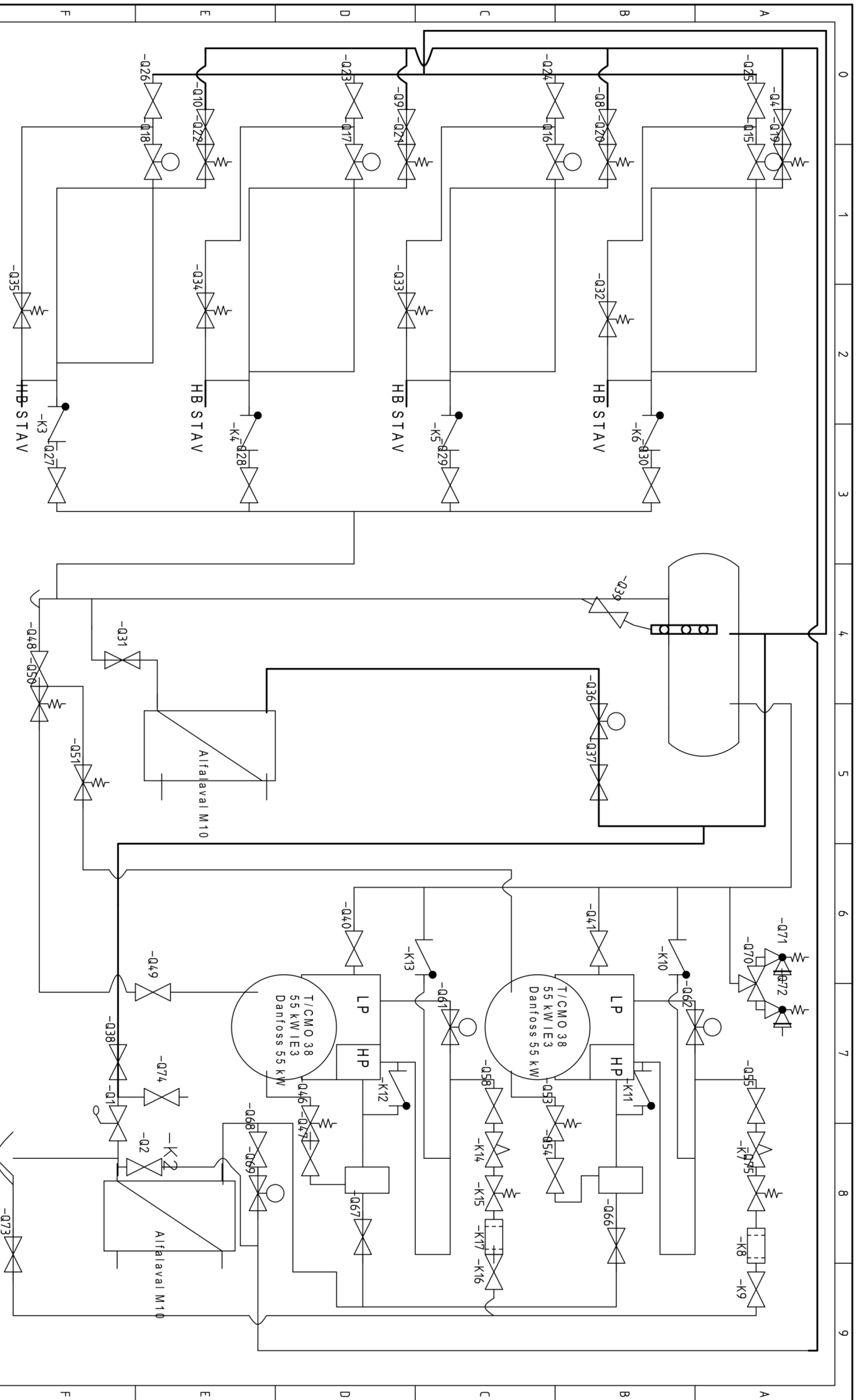
2 trins drift:

Når udetemperaturen (T5) falder under -10°C (justerbart)

Åbnes V60, V61 og V70,V71 derved går kompressorerne over i 2 trins drift

Når temperaturen stiger til -6°C (T5) (justerbart) lukkes V60, V61 og V70, V71

E PI-diagram of heat pump



FB. VEJ 40

Projekt	GK kulde Bergen	Initiater	MR	Antal sider	1
Dato	02-11-2015	Revision	1	Dokumentnummer	2015-008
				Neste side	
				Side	1

F Heat exchanger in the heat pump



Alfa Laval M10

Gasketed plate-and-frame heat exchanger for a wide range of applications

Alfa Laval Industrial line is a wide product range that is used in virtually all types of industry.

Suitable for a wide range applications, this model is available with a large selection of plate and gasket types.

In addition to normal single plate configuration, this model is also available with double wall plates. Double wall plates are used as an extra precaution to avoid intermixing of fluids.

Applications

- Biotech and Pharmaceutical
- Chemicals
- Energy and Utilities
- Food and Beverages
- Home and Personal care
- HVAC and Refrigeration
- Machinery and Manufacturing
- Marine and Transportation
- Mining, Minerals and Pigments
- Pulp and Paper
- Semiconductor and Electronics
- Steel
- Water and Waste treatment

Benefits

- High energy efficiency – low operating cost
- Flexible configuration – heat transfer area can be modified
- Easy to install – compact design
- High serviceability – easy to open for inspection and cleaning and easy to clean by CIP
- Access to Alfa Laval's global service network

Features

Every detail is carefully designed to ensure optimal performance, maximum uptime and easy maintenance. Selection of available features:

- Corner guided alignment system
- Chocolate pattern distribution area
- Glued gasket
- Clip-on gasket
- Leak chamber
- Fixed bolt head
- Key hole bolt opening
- Lifting lug
- Lining
- Lock washer
- Tightening bolt cover



Extending performance

with Alfa Laval 360° Service Portfolio

Our extensive services ensure top performance from your Alfa Laval equipment throughout its life cycle. The availability of parts and our team's commitment and expertise bring you peace of mind.

Start-up

- Installation
- Installation Supervision
- Commissioning

Maintenance

- Cleaning Services
- Reconditioning
- Repair
- Service Tools
- Spare Parts

Support

- Exclusive Stock
- Technical Documentation
- Telephone Support
- Training
- Troubleshooting

Improvements

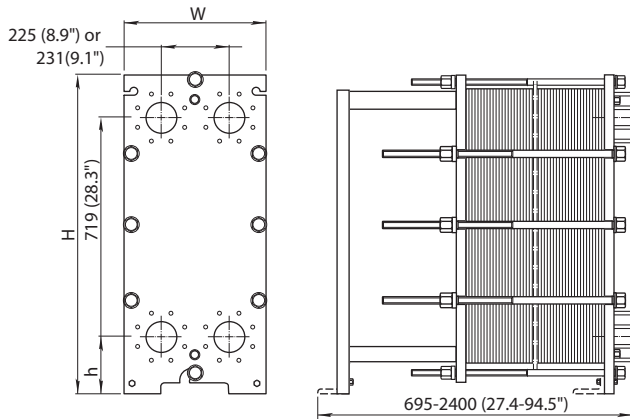
- Equipment Upgrades
- Redesign
- Replacement and Retrofit

Monitoring

- Condition Audit
- Performance Audit

Dimensional drawing

Measurements mm (inches)



Type	H	W	h
M10-FM	1084 (42.7")	470 (18.5")	215 (8.5")
M10-FG	1084 (42.7")	470 (18.5")	215 (8.5")
M10-FD	981 (38.6")	470 (18.5")	131 (5.2")
M10-FD, ASME	1084 (42.7")	470 (18.5")	215 (8.5")

The number of tightening bolts may vary depending on pressure rating.

Technical data

Plates

Name	Type	Free channel, mm (inches)
M10-B	Single plate	2.6 (0.10)
M10-M	Single plate	4.0 (0.16)
M10-MX	Single plate Diagonal flow	4.0 (0.16)
M10-BD	Double wall plate	2.6 (0.10)

Materials

Heat transfer plates	316/316L, 316Ti, 904L, 254 C-22, C-276, C-2000, D-205 B-3, G-30, 400, 625, 825 Alloy 33, Ni, Ti, TiPd
Field gaskets	NBR, EPDM, FKM, Q
Flange connections	Carbon steel Metal lined: stainless steel, titanium Rubber lined: NBR, EPDM
Frame and pressure plate	Carbon steel, epoxy painted

Other materials may be available on request.

All option combinations may not be configurable.

Operational data

Frame, PV-code	Max. design pressure (barg/psig)	Max. design temperature (°C/°F)
FL, pvcALS	6.0/87	130/266
FM, pvcALS	10.0/145	180/356
FM, PED	10.0/145	180/356
FG, pvcALS	16.0/232	180/356
FG, ASME	10.3/150	180/356
FG, PED	16.0/232	180/356
FD, pvcALS	25.0/363	180/356
FD, ASME	26.8/389	250/482

Extended pressure and temperature rating may be available on request.

The FG frame is also approved for 12 barg/200°C to allow use in steam systems without safety valves.

Flange connections

FL, pvcALS	EN 1092-1 DN100 PN10 JIS B2220 10K 100A
FM, pvcALS	EN 1092-1 DN100 PN10 ASME B16.5 Class 150 NPS 4 JIS B2220 10K 100A
FM, PED	EN 1092-1 DN100 PN10 ASME B16.5 Class 150 NPS 4
FG, pvcALS	EN 1092-1 DN100 PN16 ASME B16.5 Class 150 NPS 4 JIS B2220 10K 100A JIS B2220 16K 100A
FG, ASME	ASME B16.5 Class 150 NPS 4
FG, PED	EN 1092-1 DN100 PN16 ASME B16.5 Class 150 NPS 4
FD, ASME	ASME B16.5 Class 300 NPS 4
FD, PED	EN 1092-1 DN100 PN25 ASME B16.5 Class 150 NPS 4 ASME B16.5 Class 300 NPS 4

Standard EN1092-1 corresponds to GOST 12815-80 and GB/T 9115.

How to contact Alfa Laval

Contact details for all countries are continually updated on our website. Please visit www.alfalaval.com to access the information direct.

G Compressor in the heat pump

TCMO/TSMC two-stage reciprocating compressors

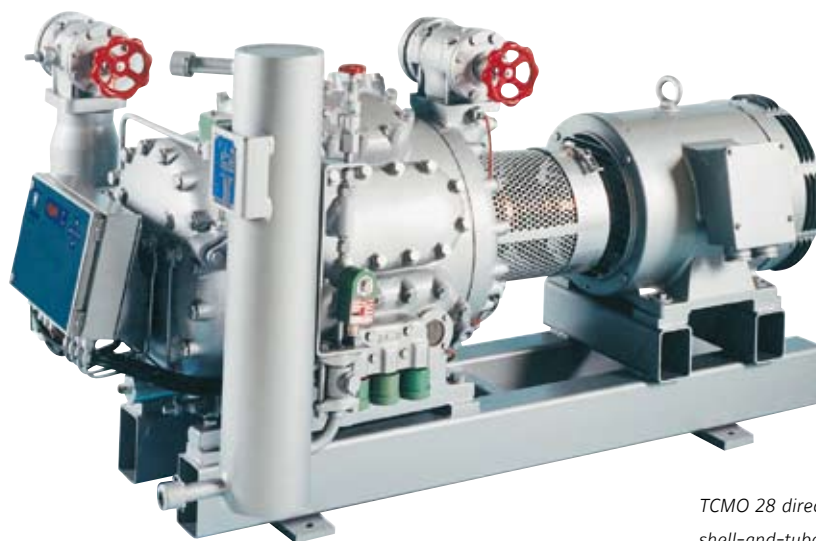
In all low-temperature refrigeration installations, two-stage reciprocating compressors are an economical operating alternative to single-stage screw compressors.

Sabroe TCMO/TSMC two-stage reciprocating compressors are therefore ideal for medium-size industrial and marine refrigeration installations. They are the most reliable and economical option for a range of heavy-duty applications on this particular scale, where an extended service life is required.

The TCMO/TSMC range includes eight two-stage models that provide capacities between 175 and 1018 m³/h low-pressure swept volume at maximum speed.

Compatible and upgradable

The Sabroe TCMO/TSMC design is future-compatible because ongoing changes and improvements are designed so that they can also be implemented on earlier TCMO/TSMC models. This makes it easy to upgrade and retrofit older compressors to the most recent specifications.



TCMO 28 direct-coupled unit with shell-and-tube intermediate cooler

Significant advantages

The advantages of the Sabroe TCMO/TSMC compressor design include

- High coefficient of performance (COP), with excellent part-load characteristics.
- Excellent accessibility – including simple-to-clean water covers and externally accessible oil pump/filter (TSMC 100 only) – and limited spare parts requirements.
- Any necessary repairs can normally be undertaken without having to remove the compressor.
- Chromium piston rings, gas-dampened discharge valves and hardened cylinder liner surfaces.
- Spring-loaded safety heads, balanced refrigerant-tight shaft seal, asbestos-free gaskets and an internal bypass valve to prevent excessive pressure.

Customer benefits

For the customer, the benefits of the Sabroe TCMO/TSMC compressor design include

- ▶ Lower power consumption, especially when operating at part load. This greatly reduces operating costs.
- ▶ Easy maintenance, resulting in low service costs and minimal downtime.
- ▶ All repairs can be carried out on site at the customer's own premises, reducing both repair costs and downtime.
- ▶ Extended service life for all moving parts.
- ▶ The special design ensures low noise and low vibration levels, with safe, environmentally responsible operation.

Standard equipment

Sabroe TCMO/TSMC compressors are supplied with the following equipment as standard

- compressor block with oil pump and oil filter
- solenoid valves for capacity control
- suction and discharge stop valves
- safety valve
- oil-charging valve
- suction filter
- oil-level sight glass
- electric immersion heater in crankcase
- evacuation valve
- pre-lubrication valve.

Optional equipment

A wide range of optional equipment is also available for Sabroe TCMO/TSMC compressors. This includes

- gauges, thermometers and temperature/pressure control switches
- Sabroe Unisab III microprocessor control with temperature/pressure sensors
- extended one-cylinder capacity control or standard capacity control with full unloading (TSMC 100 only)
- oil level regulator for parallel systems
- explosion-proof equipment
- base frame with coupling and guard for direct-drive unit
- base frame with pulleys, belts and guard for V-belt drive unit
- motors

- oil separators with solenoid valve and TLT valve (TSMC 100 only) for oil return
- oil charging pump
- vibration dampers and foundation bolts
- tool sets
- sets of genuine Sabroe spare parts.

Compressor and oil cooling

Depending on specific refrigerant and operating conditions, it can be necessary to supplement basic air convection cooling with one of the following options to make sure that the compressor and the lubricating oil are cooled efficiently

- water-cooled head covers
- water-cooled side covers for oil cooling
- refrigerant-based oil cooling
- thermo-pump system (for use with R717 only).

Intermediate cooling systems

The two-stage compressors are available for connection to a common intermediate cooler in plants with multiple two-stage compressors. Alternatively, the following intermediate cooling systems are available in built-on form, as optional equipment

- injection interstage gas cooling without liquid sub-cooling
- injection interstage gas cooling with liquid subcooling in a shell-and-tube heat exchanger
- closed flash interstage cooling in a shell-and-coil intermediate cooler with liquid subcooling in the coil.

Model	Number of cylinders low/high-pressure side	Bore x stroke mm	Max. rpm	Low-pressure side swept volume at max. rpm, m ³ /h	Normal capacities in kW at 1500 rpm				Dimensions in mm Direct-coupled unit without intermediate cooler			Weight excl. motor kg	Sound pressure level dB(A)
					-40/+35°C				L	W	H		
					R717	R134a	R404A	R507					
TCMO 28	6 / 2	70 x 70	1800	175	20	11	27	28	1400-1750	700	1000	500	71
TCMO 38	6 / 2	70 x 82	1800	204	23	14	32	33	1400-1750	700	1000	500	71
TSMC 108 S	6 / 2	100 x 801	1500	339	50	30	66	70	1900-2500	1050	1125	1000	82
TSMC 108 L	6 / 2	100 x 100	1500	424	66	31 *)	68 *)	72 *)	1900-2500	1050	1125	1000	83
TSMC 108 E	6 / 2	100 x 120	1500	509	82	NA	NA	NA	1900-2500	1050	1125	1000	83
TSMC 116 S	12 / 4	100 x 801	1500	669	100	60	132	139	2475-3200	1150	1335	1800	84
TSMC 116 L	12 / 4	100 x 100	1500	848	133	62 *)	136 *)	144 *)	2475-3200	1150	1335	1800	84
TSMC 116 E	12 / 4	100 x 120	1500	1018	163	NA	NA	NA	2475-3200	1150	1335	1800	84

Nominal capacities are based on 2°C subcooling from condenser, 2°C superheat and liquid subcooling in intermediate cooler to 10°C above intermediate temperature.
Nominal capacities are at max. rpm except for: *) at 1200 rpm

All information is subject to change without previous notice

Johnson Controls Denmark ApS · Sabroe Products
Christian X's Vej 201 · 8270 Højbjerg · Denmark
Phone +45 87 36 70 00 · Fax +45 87 36 70 05
www.sabroe.com



H Risk assessment

Unit:	NTNU	Risk assessment	Prepared by	Number	Date	
			HSE section	HMSRV/2603E	04.02.2011	
	HSE/KS		Approved by		Replaces	
			The Rector		01.12.2006	

Department of Energy and Process Engineering

Date: 14.01.2019

Line manager: Armin Hafner **Participants in the identification process** (including their function): Lars-Adrian Amundsen (Student)

Short description of the main activity/main process: Master project for student Lars-Adrian Amundsen. Evaluation of a reversible NH3 heat pump.

Signatures: Responsible supervisor: 



Student: 

Activity from the identification process form	Potential undesirable incident/strain	Likelihood:	Consequence:			Risk Value (human)	Comments/status Suggested measures
		Likelihood (1-5)	Human (A-E)	Environment (A-E)	Economy/material (A-E)		
1	Leakage	2	B	A	B	B2	Gas sensors are installed. Gas alarm. Emergency exit is clearly marked. Gas mask available.

Likelihood, e.g.:

Consequence, e.g.:

Risk value (each one to be estimated separately):

NTNU	Risk assessment	Prepared by	Number	Date	
		HSE section	HMSRV2603E	04.02.2011	
HSE/KS		Approved by		Replaces	
		The Rector		01.12.2006	

- | | | |
|---|---|---|
| 1. <i>Minimal</i>
2. <i>Low</i>
3. <i>Medium</i>
4. <i>High</i>
5. <i>Very high</i> | A. <i>Safe</i>
B. <i>Relatively safe</i>
C. <i>Dangerous</i>
D. <i>Critical</i>
E. <i>Very critical</i> | Human = Likelihood x Human Consequence
Environmental = Likelihood x Environmental consequence
Financial/material = Likelihood x Consequence for Economy/materiel |
|---|---|---|

Potential undesirable incident/strain

Identify possible incidents and conditions that may lead to situations that pose a hazard to people, the environment and any materiel/equipment involved.

Criteria for the assessment of likelihood and consequence in relation to fieldwork

Each activity is assessed according to a worst-case scenario. Likelihood and consequence are to be assessed separately for each potential undesirable incident. Before starting on the quantification, the participants should agree what they understand by the assessment criteria:



Likelihood

Minimal 1	Low 2	Medium 3	High 4	Very high 5
Once every 50 years or less	Once every 10 years or less	Once a year or less	Once a month or less	Once a week

Consequence

Grading	Human	Environment	Financial/material
E Very critical	May produce fatality/ies	Very prolonged, non-reversible damage	Shutdown of work >1 year.
D Critical	Permanent injury, may produce serious serious health damage/sickness	Prolonged damage. Long recovery time.	Shutdown of work 0.5-1 year.
C Dangerous	Serious personal injury	Minor damage. Long recovery time	Shutdown of work < 1 month
B Relatively safe	Injury that requires medical treatment	Minor damage. Short recovery time	Shutdown of work < 1 week
A Safe	Injury that requires first aid	Insignificant damage. Short recovery time	Shutdown of work < 1 day

The unit makes its own decision as to whether opting to fill in or not consequences for economy/materiel, for example if the unit is going to use particularly valuable equipment. It is up to the individual unit to choose the assessment criteria for this column.

NTNU	Risk assessment	Prepared by	Number	Date	
		HSE section	HMSRV/2603 E	04.02.2011	
HSE/KS		Approved by		Replaces	
		The Rector		01.12.2006	

Risk = Likelihood x Consequence

Please calculate the risk value for "Human", "Environment" and, if chosen, "Economy/materiel", separately.

About the column "Comments/status, suggested preventative and corrective measures":

Measures can impact on both likelihood and consequences. Prioritise measures that can prevent the incident from occurring; in other words, likelihood-reducing measures are to be prioritised above greater emergency preparedness, i.e. consequence-reducing measures.

NTNU	Risk matrix	prepared by	Number	Date	
		HSE Section	HMSRV/2604	March 2010	
HSE/KS		approved by	Page	Replaces	
	Rector	of 4	February 2010		

MATRIX FOR RISK ASSESSMENTS at NTNU

CONSEQUENCE	Extremely serious	E1	E2	E3	E4	E5
	Serious	D1	D2	D3	D4	D5
	Moderate	C1	C2	C3	C4	C5
	Minor	B1	B2	B3	B4	B5
	Not significant	A1	A2	A3	A4	A5
		Very low	Low	Medium	High	Very high
		LIKELIHOOD				

Principle for acceptance criteria. Explanation of the colours used in the risk matrix.

Colour	Description
Red	Unacceptable risk. Measures must be taken to reduce the risk.
Yellow	Assessment range. Measures must be considered.

Green

Acceptable risk Measures can be considered based on other considerations.

